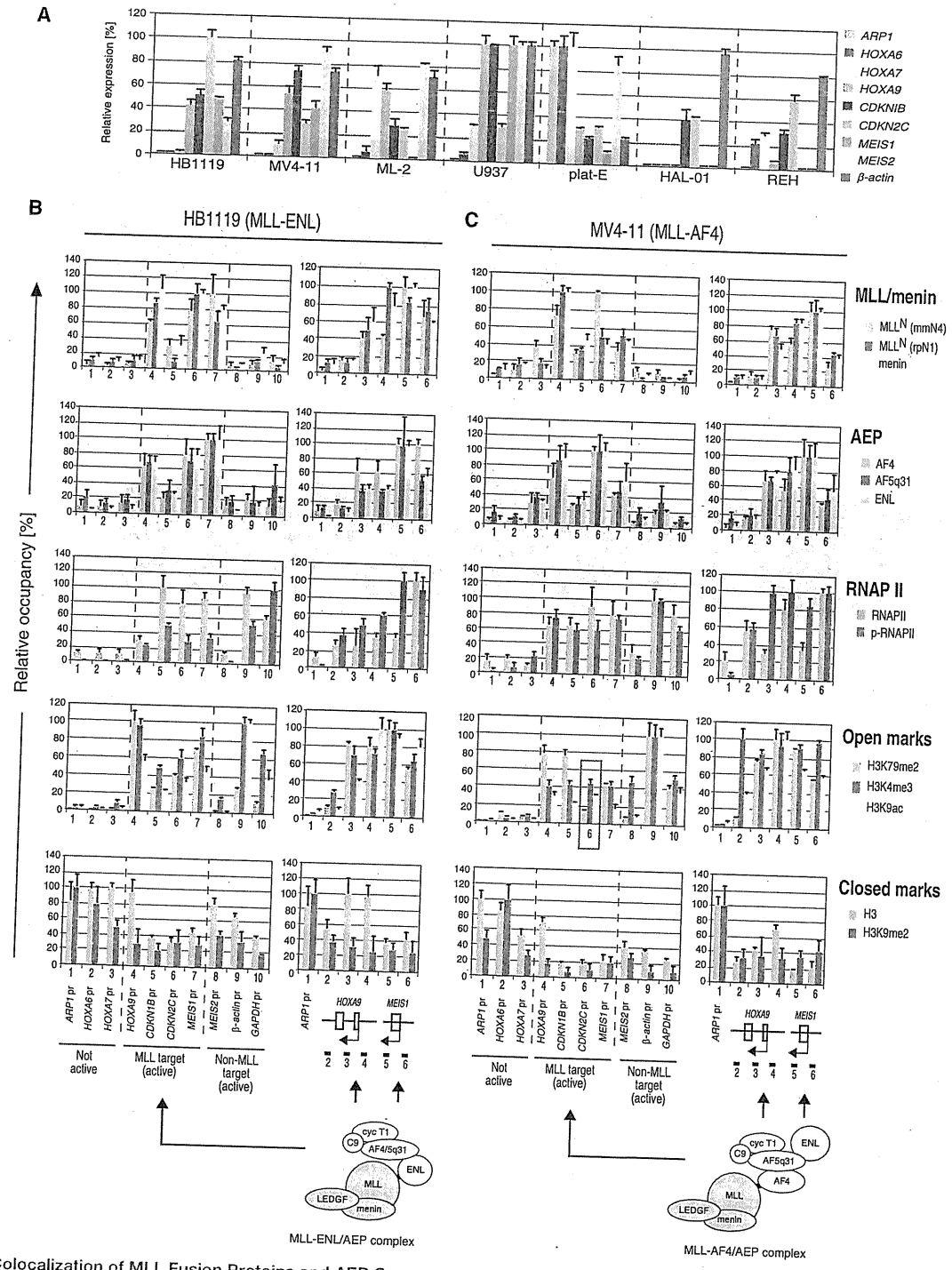

Figure 2. Colocalization of MLL Fusion Proteins and AEP Components on Chromatin

(A) Relative expression of various genes (indicated on the right) in seven human cell lines was analyzed by quantitative RT-PCR. Expression levels were normalized to *GAPDH* and are depicted relative to the highest value among the seven cell lines arbitrarily set as 100. Error bars represent standard deviations of triplicate PCRs.

(B) Genomic localizations of various proteins in HB1119 cells were determined by ChIP assay. Cross-linked chromatin was immunoprecipitated with antibodies specific for the indicated proteins and analyzed by quantitative PCR using primer/probe sets that target promoter-adjacent regions or other genomic regions indicated at the bottom. Occupancies are displayed relative to the highest value in the group arbitrarily set as 100. Error bars represent standard deviations of triplicate PCRs. Genes expressed more than 20% of the highest levels in (A) are defined as active genes.

(C) A comparable analysis as in (B) was performed for MV4-11 cells, which harbor a t(4;11) translocation and express MLL-AF4 proteins. The purple rectangle highlights a locus on which dimethyl H3K79 marks were absent, but the MLL-AF4/AEP complex was present. See also Figure S2.

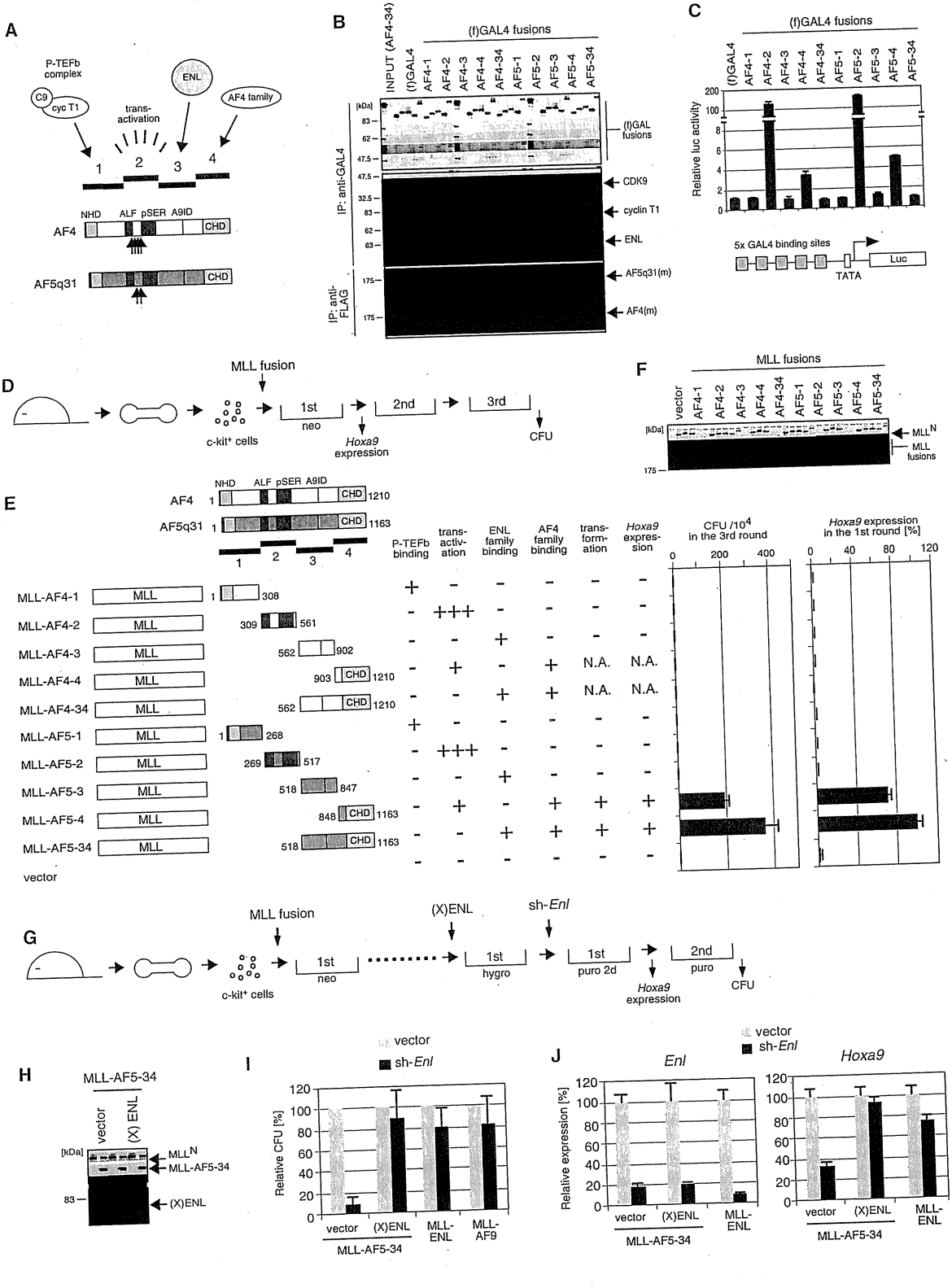
A
P-TEFb complex
C9
cyc T1
ENL
AF4 family
trans-activation
1
2
3
4
NHD
ALF
pSER
A9ID
AF4
CHD
AF5q31
B
INPUT (AF4-34)
(f)GAL4
(f)GAL4 fusions
AF4-1
AF4-2
AF4-3
AF4-4
AF4-34
AF5-1
AF5-2
AF5-3
AF5-4
AF5-34
[kDa]
IP: anti-GAL4
IP: anti-FLAG
(f)GAL fusions
CDK9
cyclin T1
ENL
AF5q31(m)
AF4(m)
C
Relative luc activity
5x GAL4 binding sites
Luc
TATA
D
MLL fusion
c-kit+ cells
1st
neo
2nd
3rd
Hoxa9 expression
CFU
F
MLL fusions
vector
MLL^N
MLL fusions
E
AF4
AF5q31
MLL-AF4-1
MLL-AF4-2
MLL-AF4-3
MLL-AF4-4
MLL-AF4-34
MLL-AF5-1
MLL-AF5-2
MLL-AF5-3
MLL-AF5-4
MLL-AF5-34
vector
P-TEFb binding
trans-activ-ation
ENL family binding
AF4 family binding
trans-form-ation
Hoxa9 expres-sion
N.A.
CFU /10^4 in the 3rd round
Hoxa9 expression in the 1st round [%]
G
MLL fusion
(X)ENL
sh-Enl
c-kit+ cells
1st
neo
1st
hygro
1st
puro 2d
2nd
puro
Hoxa9 expression
CFU
H
MLL-AF5-34
vector
(X) ENL
[kDa]
MLL^N
MLL-AF5-34
(X)ENL
I
vector
sh-Enl
Relative CFU [%]
vector
(X)ENL
MLL-ENL
MLL-AF9
MLL-AF5-34
J
Enl
Hoxa9
vector
sh-Enl
Relative expression [%]
vector
(X)ENL
MLL-ENL
MLL-AF5-34

Anc1 (designated AHD: Anc1 homology domain), displayed transactivation potential that correlated with association with AF4 family proteins (Figure 4C). The AHD of ENL also mediated association with DOT1L (Figure 4D), consistent with results of previous studies (Mueller et al., 2007). Mutations of MLL-ENL that abolished AF5q31 and DOT1L interaction (including a single L550E point mutation) resulted in failure to up-regulate *Hoxa9* transcription and transform myeloid progenitors (Figures 4E–4G). Similarly, the portion of AF9 retained in MLL-AF9 oncoproteins, which includes AHD (residues 502–568) (Figure 4A), mediated AF5q31 and DOT1L association and conferred GAL4-dependent transactivation, MLL-dependent *Hoxa9* expression, and myeloid transformation (Figures 4B–4G). Unlike MLL-AF5q31-transformed cells, MLL-ENL- and MLL-AF9-transformed cells did not require WT Enl because their clonogenicities were unaffected by its knockdown (Figures 3I and 3J), consistent with the observation that MLL-ENL did not form a complex with WT ENL in HB1119 cells (Figure 1E). These results suggest that association with AF4 family proteins and/or DOT1L is required for the oncogenic properties of MLL-ENL and MLL-AF9.

Interactions of ENL with DOT1L or AF4 Family Proteins Are Mutually Exclusive

To determine whether ENL can simultaneously coassociate with AF4 family proteins and DOT1L, IP analysis was performed on cells transiently expressing ENL, AF5q31, and DOT1L. Although ENL coprecipitated both AF5q31 and DOT1L, the latter two did not pull down each other (Figure 5A), indicating that the three proteins do not form a trimeric complex. Similarly, GAL4-AF5-3 effectively coprecipitated ENL but not DOT1L under conditions where GAL4-ENL successfully pulled down DOT1L (Figure S4). These data demonstrate that the associations of ENL family proteins with AF4 family proteins or DOT1L are mutually exclusive. Therefore, the ENL/DOT1L complex is a separate entity from AEP (Figure 5B).

Recruitment of AEP, versus DOT1L, Plays a Predominant Role in MLL-Dependent Leukemogenesis

The ability of MLL-ENL to associate with AF4 family proteins or DOT1L raised the issue of which interaction (MLL-ENL/AEP vs. MLL-ENL/DOT1L) is essential for leukemic transformation (Figure 5B). To address this issue, an artificial MLL fusion with DOT1L (MLL-DOT1L) that does not associate with AF4 (Figure 5C) but retains the HMT catalytic domain (thus mimics the MLL-ENL/DOT1L complex) was assessed for its transformation potential. MLL-DOT1L failed to sufficiently activate *Hoxa9* expression to immortalize myeloid progenitors (Figures 5D and 5E), despite the comparable levels of protein expression in packaging cells (Figure 5F) and mRNA expression in first-round colonies (Figure 5E). In the same experimental condition, MLL-AF5q31 successfully transformed myeloid progenitors (Figure 5E) without being able to directly associate with DOT1L (Figure 5C). These results, which contrast with those of previous studies (Okada et al., 2005), indicate that simple recruitment of DOT1L HMT activity alone to MLL target genes is not sufficient for transformation and support a more predominant role for AEP recruitment.

Nevertheless, DOT1L-dependent H3K79 methylation colocalized with the presence of MLL-ENL at all target loci tested in HB1119 cells (Figure 2B), indicating that not only AEP components but also DOT1L is consistently recruited by MLL-ENL. In MV4-11 cells, H3K79 methylation marks also colocalized at most of the MLL-AF4-occupied loci, consistent with previous observations (Krivtsov et al., 2008; Guenther et al., 2008), despite the apparent inability to directly recruit DOT1L (Figures 2C and 5C). However, the signal intensities of H3K79 dimethylation were relatively low at MLL-AF4-target loci, compared with those at MLL-ENL-target loci (compare relative intensities to those of *β-ACTIN* and *GAPDH*, which served as internal standards) (Figures 2B and 2C; Figure S2) and were minimal at the *CDKN2C* promoter in spite of the localization of abundant AEP components (Figure 2C, purple rectangle). Thus, DOT1L-dependent

Figure 3. Formation of an AEP-Like Complex Is Required for MLL-AF5q31-Dependent Myeloid Transformation

(A) The structures of AF4 and AF5q31 are schematically illustrated. Subregions (1–4) of AF4 and AF5q31 are indicated with associated functions. Upward arrows indicate the sites of fusion with MLL in human leukemia oncoproteins (Jansen et al., 2005) (A9ID, AF9 interaction domain; Srinivasan et al., 2004).

(B) The four subregions fused to GAL4 DNA binding domain were expressed in 293T cells (upper four panels) or coexpressed with myc-tagged AF4 or AF5q31 [AF4(m) or AF5q31(m)] (lower two panels) and analyzed by IP western blotting. IP antibodies are indicated on the left and proteins detected by western blotting are indicated on the right. (f)GAL4 fusions and myc-tagged AF4 family proteins were visualized with anti-FLAG and anti-myc antibodies, respectively.

(C) Transactivation activity of respective GAL4 fusions was analyzed using the reporter gene shown below. Error bars represent standard deviations from triplicate analyses.

(D) The experimental scheme of myeloid progenitor transformation assays to evaluate the oncogenic potentials of various MLL mutants shows the time points at which CFU (colony forming unit) activity or *Hoxa9* expression was examined.

(E) The structures of various MLL-AF4/AF5q31 mutants and their associated functions are summarized schematically. *Hoxa9* levels were normalized to *Gapdh* and displayed relative to *MLL-AF5-34*-transduced cells arbitrarily set at 100%. Error bars represent standard deviations of three independent analyses (left) or triplicate PCRs (right). N.A., not applicable because of unstable expression of MLL fusion proteins.

(F) Protein levels of respective MLL mutants in virus-packaging cells were examined by western blotting with anti-MLL^N antibody. MLL-AF4-4 and MLL-AF4-34 proteins were not stably expressed.

(G) The experimental scheme to evaluate the effect of *Enl* knockdown on MLL transformation is shown schematically. (X)ENL, Xpress-tagged human ENL.

(H) Transduced myeloid progenitors were analyzed by western blotting with anti-MLL^N (top) and anti-Xpress (bottom) antibodies to detect exogenous MLL-AF5q31 and human (X)ENL, respectively.

(I) The clonogenic potentials of MLL-AF5-34-transformed cells transduced with or without *(X)ENL* are shown at the second plating after sh-RNA transduction (vector or sh-*Enl*). MLL-ENL- or MLL-AF9-transformed cells were also subjected to sh-RNA transduction for comparison. CFUs are expressed relative to the vector control arbitrarily set as 100. Error bars represent standard deviations of three independent analyses.

(J) Cells from first-round colonies following sh-RNA transduction (vector or sh-*Enl*) were analyzed by RT-PCR for expression of endogenous *Enl* or *Hoxa9*. Expression levels were normalized to *Gapdh* and displayed relative to the vector/vector control cells arbitrarily set at 100. Error bars represent standard deviations of triplicate PCRs. See also Figure S3.

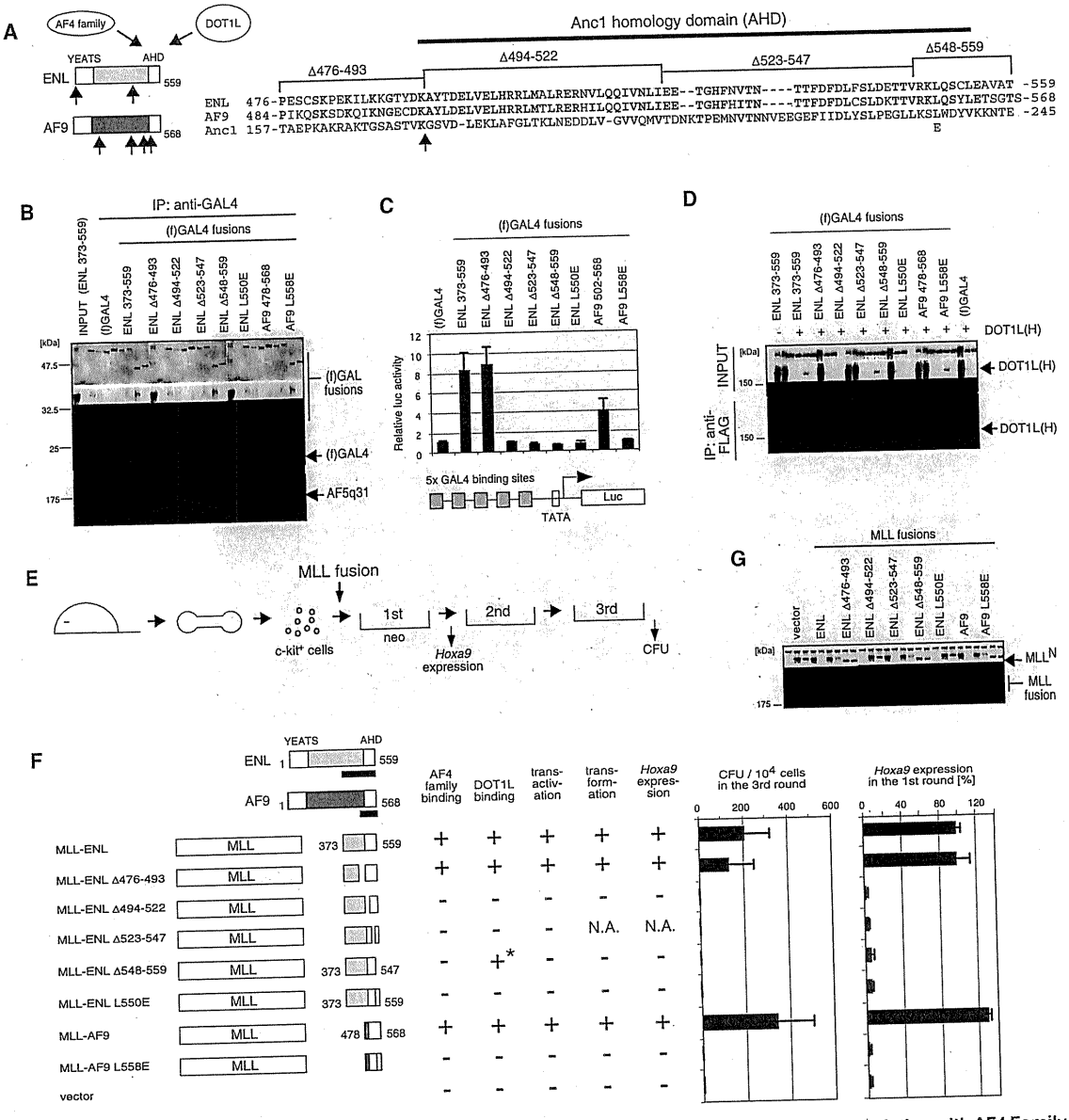

Figure 4. MLL-ENL and MLL-AF9 Transform Myeloid Progenitors via the AHD, which Is Responsible for Association with AF4 Family Proteins and DOT1L

(A) The structures of ENL and AF9 are schematically illustrated with associated functions (Zeisig et al., 2005). Aligned amino acid sequences for the minimum transformation domain are also shown with the positions of deletion or substitution mutations and AHD. Upward arrows indicate the sites of fusion with MLL in human leukemia oncoproteins (Jansen et al., 2005).

(B) Domain mapping of ENL family proteins for association with AF5q31 was performed with FLAG-tagged GAL4 fusion constructs of ENL (372–559 aa) and AF9 (478–568 aa). IP was performed with anti-GAL4 antibody, and the precipitates were immunoblotted with anti-FLAG antibody for (f)GAL4 fusions or anti-AF5q31 antibody for endogenous AF5q31.

(C) Transactivation activity of indicated GAL4 constructs was analyzed by luciferase assay as in Figure 3C.

(D) The same set of GAL4 fusion proteins used in (B) and HA-tagged DOT1L [DOT1L(H)] were coexpressed in 293T cells and analyzed by IP western blotting. IP was performed with anti-FLAG antibody and the precipitates were immunoblotted with anti-HA antibody.

(E) The experimental scheme is shown for myeloid progenitor transformation assays to evaluate the oncogenic potentials of MLL mutants.

(F) The structures of MLL-ENL and MLL-AF9 mutants and their associated functions are summarized with schematic representations. *Hoxa9* expression levels were normalized to *Gapdh* and displayed relative to the *MLL-ENL*-transduced cells arbitrarily set at 100%. Error bars represent standard deviations of three independent analyses (left) or triplicate PCRs (right). N.A., not applicable because of unstable expression of MLL fusion proteins. The asterisk indicates that association of ENL Δ548–559 mutant with DOT1L was detected but reduced substantially, compared with WT ENL.

(G) Protein levels of respective MLL mutants in virus packaging cells were examined by western blotting with anti-MLL^N antibody. MLL-ENL Δ523–547 was not stably expressed.

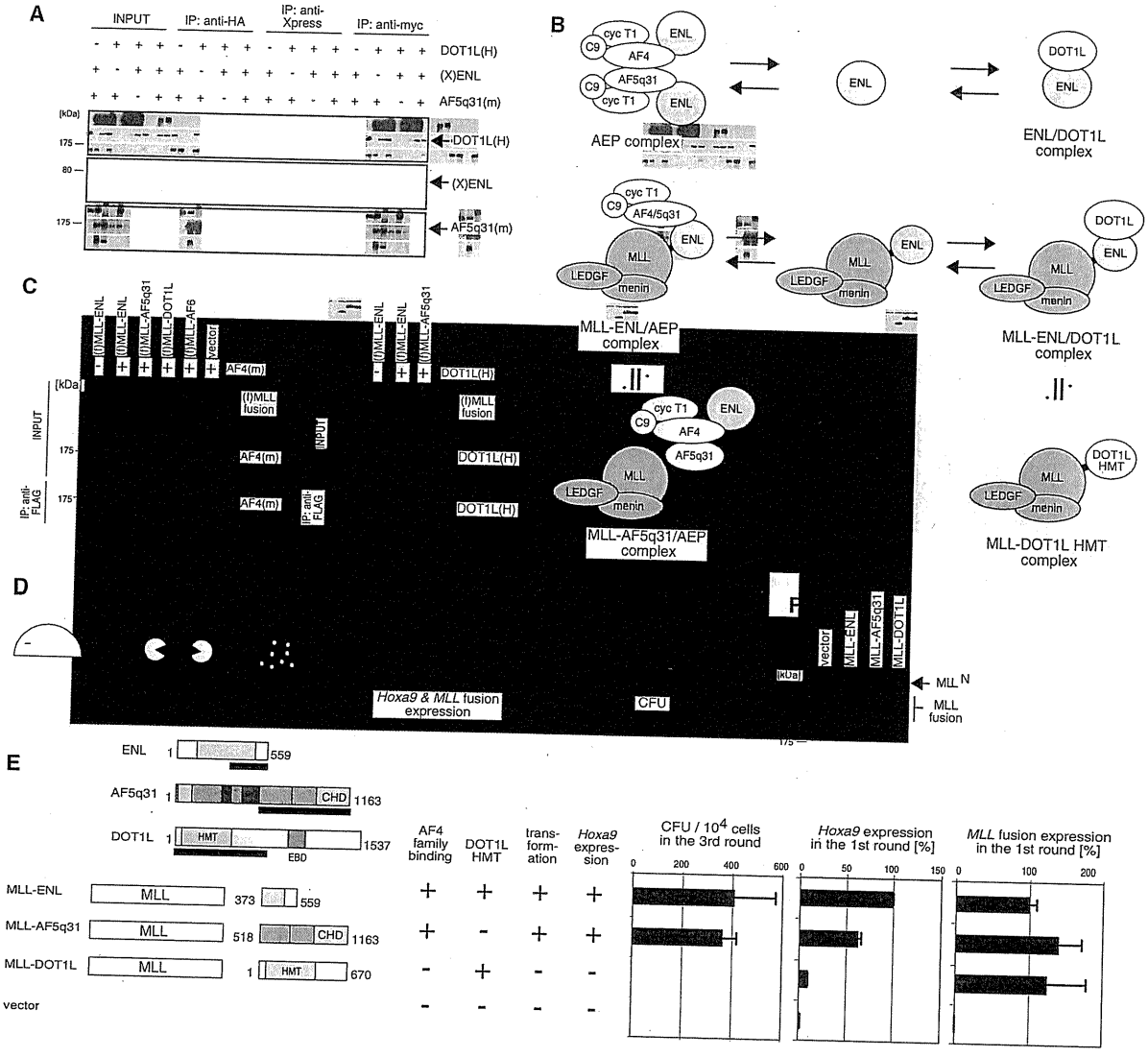

Figure 5. Associations of ENL Family Proteins with AF4 Family Proteins or DOT1L Are Mutually Exclusive

(A) AF5q31(m), (X)ENL, and DOT1L(H) were coexpressed in 293T cells and analyzed by IP western blotting. IP was performed with antibodies indicated on the top, and the precipitates were immunoblotted with anti-myc, anti-Xpress, or anti-HA antibody.

(B) Putative conformations of various ENL complexes are shown schematically. ENL forms two distinct complexes: AEP and ENL/DOT1L. Similarly, MLL-ENL participates in two mutually exclusive associations to form the MLL-ENL/AEP and MLL-ENL/DOT1L complexes that are approximate to the MLL-AF5q31/AEP and MLL-DOT1L complexes, respectively.

(C) FLAG-tagged MLL fusion proteins [(f) MLL fusions] were coexpressed with AF4(m) or DOT1L(H) in 293T cells and were analyzed by IP western blotting. IP was performed with anti-FLAG antibody, and the precipitates were immunoblotted with anti-MLL^N, anti-myc, or anti-HA antibody.

(D) The experimental scheme is shown for myeloid progenitor transformation assays to evaluate the oncogenic potentials of MLL mutants.

(E) The structures of MLL-fusion proteins and their associated functions are summarized. Expression of *MLL* fusion genes or *Hoxa9* was examined by RT-PCR in first-round colonies. Expression levels were normalized to *Gapdh* levels and are displayed relative to the transcript levels in *MLL-ENL*-transduced cells arbitrarily set at 100. Error bars represent standard deviations of three independent analyses (left) or triplicate PCRs (middle and right). HMT, histone methyltransferase catalytic domain; EBD, ENL binding domain (Okada et al., 2005; Mueller et al., 2007).

(F) Protein levels of MLL fusions in virus packaging cells were analyzed by western blotting with anti-MLL^N antibody. See also Figure S4.

H3K79 methylation is associated with the presence of the MLL-AF4/AEP-hybrid complex, but the two distinct biochemical entities are not constitutively coupled. These results suggest that DOT1L is functionally linked to MLL-AF4 but normally recruited to target loci subsequent to AEP components.

AEP Is Indirectly Recruited to MLL-AF6-Occupied Loci to Sustain Transcription and Transformation

To investigate whether AEP involvement is restricted to MLL fusions with AF4 and ENL family proteins, ChIP analyses were performed on ML-2 cells. Surprisingly, MLL-AF6 colocalized

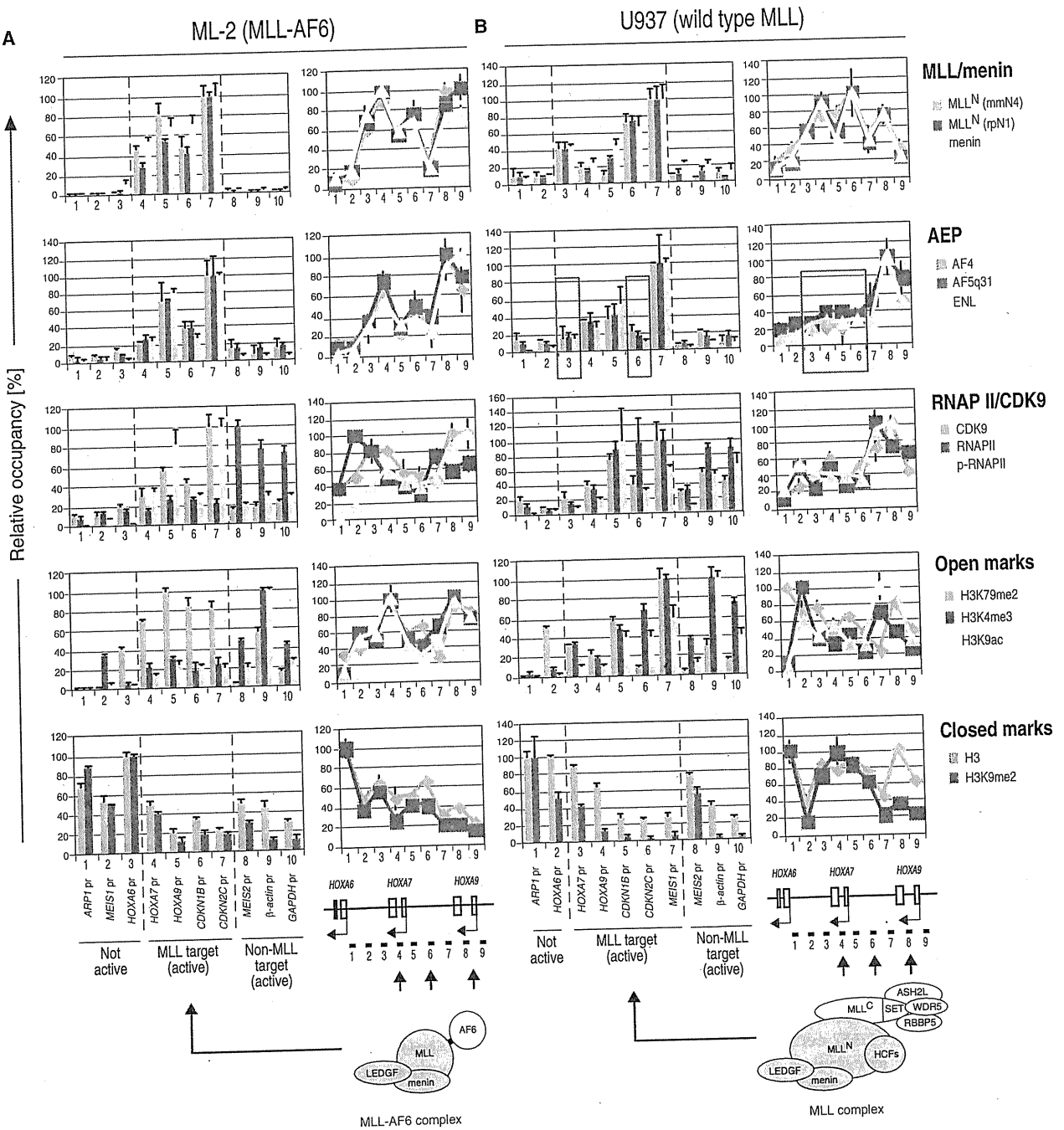

Figure 6. Indirect Recruitment of AEP to MLL-AF6- or WT MLL-Occupied Loci

(A and B) Genomic localizations of indicated proteins in ML-2 (A) and U937 (B) cells were determined by ChIP assay as in Figure 2B. The purple rectangle highlights regions where AEP is absent while the MLL complexes are present. ChIP data using anti-MLL^N (rpN1) and anti-menin antibodies are partially adapted from a previous report (Yokoyama and Cleary, 2008). See also Figure S5.

with AEP at the chromatin of MLL target genes (*HOXA7*, *HOXA9*, *CDKN1B*, and *CDKN2C*) (Figure 6A and Figure S5A) despite its inability to directly associate with AEP (Figures 1E and 5C). The occupancies of CDK9 and phosphorylated RNAPII coincided with the presence of AEP on MLL-AF6 target genes (Figure 6A). Characteristically, high levels of dimethyl H3K79 were associated with the presence of AEP, corroborating the functional link between AEP and DOT1L. These results suggest

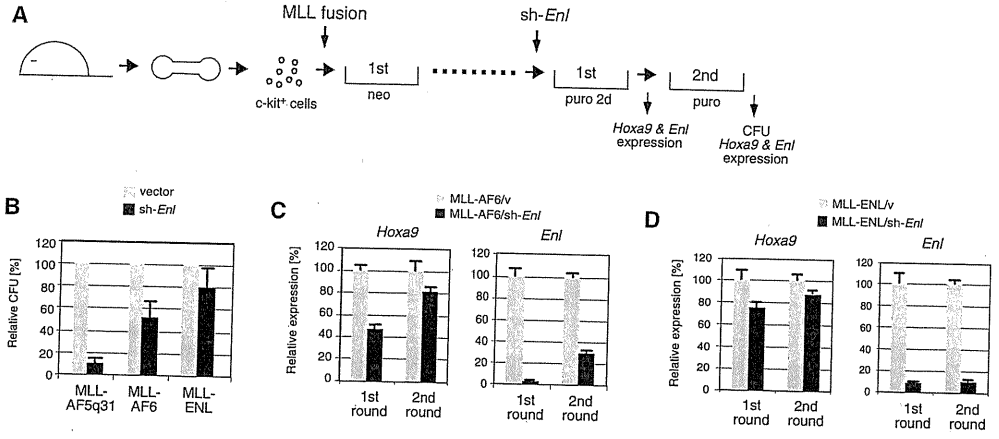

Figure 7. ENL Is Required for MLL-AF6-Dependent Transactivation and Transformation

(A) The experimental scheme to evaluate the effect of *Enl* knockdown on MLL transformation is shown.

(B) Clonogenic potentials are shown for myeloid cells transformed by MLL oncogenes (indicated below) at the second plating after sh-RNA transduction (vector or sh-*Enl*). CFU numbers are displayed relative to the vector control arbitrarily set as 100. Error bars represent standard deviations of three independent analyses.

(C) MLL-AF6-transformed cells from first- and second-round colonies following sh-RNA transduction (vector or sh-*Enl*) were analyzed by RT-PCR for expression of endogenous *Enl* or *Hoxa9*. Expression levels were normalized to *GAPDH* levels and are displayed relative to the transcript levels in vector control cells arbitrarily set as 100. Error bars represent standard deviations of triplicate PCRs.

(D) The same analysis as (C) was performed on MLL-ENL-transformed cells. Note that data in (B) and (D) are partially redundant with Figures 3I and 3J.

that the AEP complex can be recruited to MLL target loci via an indirect mechanism potentially serving a role in MLL-AF6-dependent leukemogenesis.

MLL-AF6-transformed cells were also dependent on Enl, because its knockdown reduced their clonogenicity and *Hoxa9* expression by 50% (Figures 7A and 7C). This was less severe, compared with MLL-AF5q31-transformed cells (Figure 7B), in part because of insufficient knockdown by the sh-RNA, since secondary colonies expressed *Hoxa9* at its normal levels accompanied with impaired knockdown of *Enl* (Figure 7C), indicating a selective proliferative advantage of cells in which *Enl* was incompletely knocked down (MLL-ENL served as a negative control in Figure 7D). Thus, transformation by MLL-AF6 is dependent on ENL, despite an inability to directly associate with AEP.

AEP Facilitates the Physiologic MLL-Dependent Transcriptional Pathway

The foregoing results prompted studies of a potential relationship of AEP in physiologic transcriptional regulation by WT MLL. ChIP analyses of U937 cells, which lack an MLL chromosomal translocation (Dreyling et al., 1996; Guenther et al., 2005), showed that AEP colocalized with WT MLL at the *HOXA9*, *MEIS1*, and *CDKN1B* promoters (Figure 6B and Figure S5B). However, in contrast to MLL leukemia cell lines, colocalization was not observed at all of the MLL-occupied loci in U937 cells. For instance, the MLL complex occupied both the *HOXA7* and *HOXA9* loci, whereas AEP associated only with the latter (Figure 6B, purple rectangle). A similar disparity was observed at the *CDKN2C* promoter. These results suggest that AEP is recruited to WT MLL-occupied loci in a context-dependent manner, as opposed to its constitutive recruitment in MLL leukemia cells. The presence of AEP correlated more closely with active transcriptional marks such as phospho-RNAPII and acetyl-histone H3K9 (e.g., the *HOXA7-9* locus), suggesting that AEP recruitment to MLL-targeted chromatin facilitates transcription.

The role of ENL in physiologic MLL-dependent transcriptional maintenance was assessed by knocking down *Enl* in mouse embryonic fibroblasts (MEFs), in which *Hoxc8* is a target gene of the Mll/menin complex (Figure 8A) (Hughes et al., 2004; Milne et al., 2002). *Enl* knockdown caused reduction of *Hoxc8* expression, which could be prevented by antecedent expression of exogenous human ENL (Figure 8B). Thus, Enl is required for physiologic transcriptional regulation by the Mll/menin complex. Moreover, Dot1l-mediated histone methylation was decreased at the Hoxc8 promoter in *Men1* null MEFs (Figure 8C), indicating that the MLL/menin complex functions upstream of ENL/DOT1L functions.

Furthermore, *ENL* knockdown in U937 cells caused downregulation of *HOXA9*, *CDKN1B*, and *MEIS1*, whose genomic loci were occupied by both MLL and AEP complexes, but did not affect expression of genes occupied by the MLL complex without AEP (*HOXA7* and *CDKN2C*) (*AF5q31*, *MLL*, or *β-ACTIN* served as negative controls) (Figures 6B and 8D). Thus, ENL is specifically required for the optimal transcription of genes occupied by both MLL and AEP complexes.

DISCUSSION

Our biochemical purification of AF4 family proteins demonstrates that they normally associate with ENL and the P-TEFb elongation factor in an endogenous complex (AEP) in hematopoietic cells. MLL oncoproteins fused with AEP components (AF4 or ENL family proteins) nucleate formation of MLL/AEP hybrid complexes that constitutively occupy MLL-target chromatin. This aberrant recruitment of AEP components causes sustained activation of MLL target gene transcription and transformation of hematopoietic progenitors. Although the AEP and

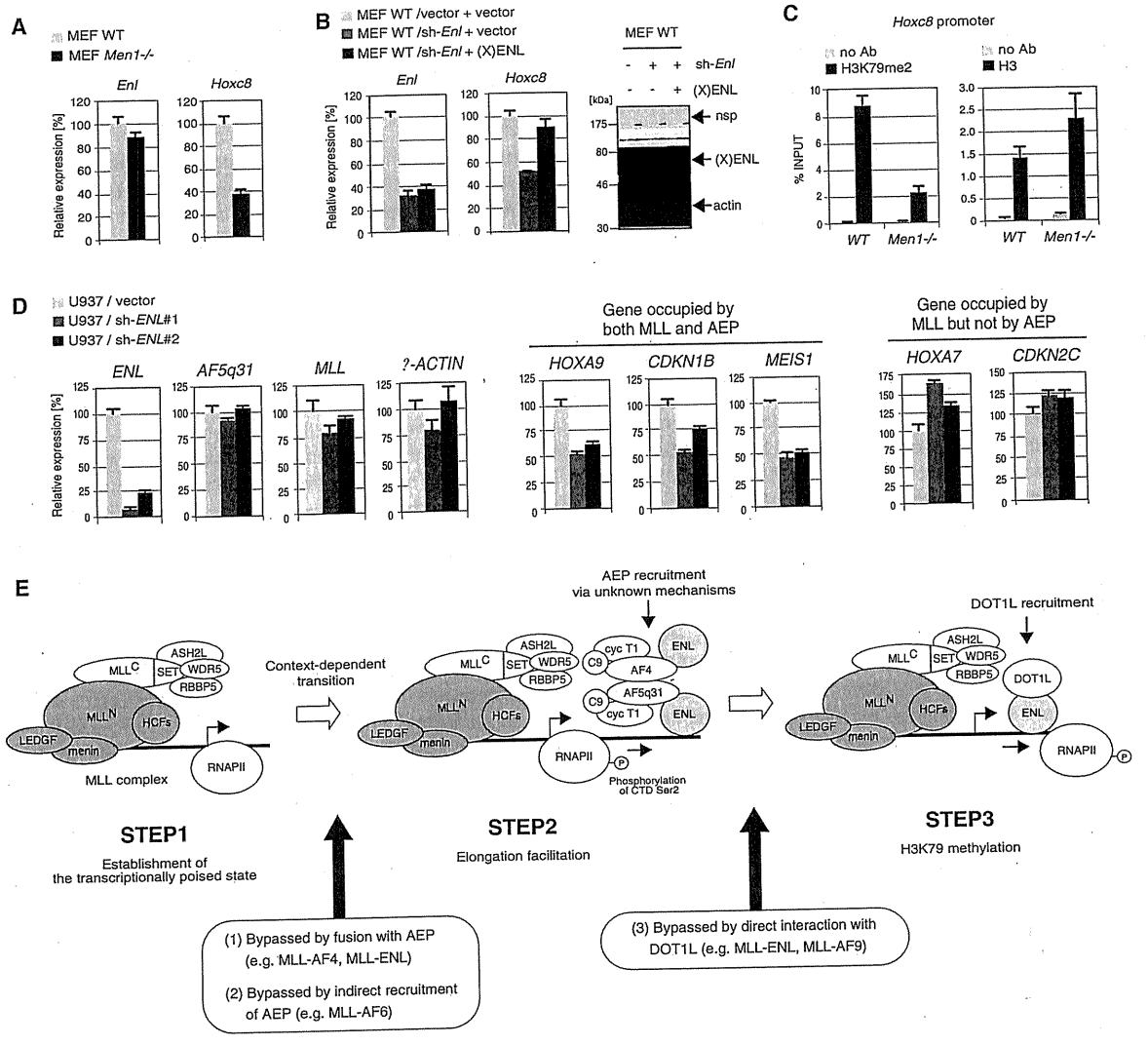

Figure 8. ENL Functions Downstream of Physiologic MLL-Dependent Transcriptional Pathways

(A) Expression levels of *Enl* and *Hoxc8* in WT or *Men1*$^{-/-}$ MEFs were determined by RT-PCR (normalized to *β-actin* levels and are displayed relative to the vector control arbitrarily set as 100). Error bars represent standard deviations of triplicate PCRs.

(B) Expression of *Enl* and *Hoxc8* with or without *Enl* knockdown/rescue was determined by RT-PCR. Expression levels were normalized to *β-actin* levels and are expressed relative to the vector/vector control arbitrarily set as 100. Error bars represent standard deviations of triplicate PCRs. Protein levels of the exogenously expressed (X)ENL (right panels) were assessed by western blotting with an anti-Xpress antibody (actin immunoblot served as a loading control). nsp, nonspecific band.

(C) ChIP assay was performed on WT or *Men1*$^{-/-}$ MEFs using anti-dimethyl H3K79 and histone H3 antibodies for the *Hoxc8* promoter-adjacent region and results displayed as relative ratio (%) to the input DNA. Error bars represent standard deviations of triplicate PCRs.

(D) The effects of *ENL*-knockdown are shown for two different sh-RNAs in U937 cells. Expression of various genes was analyzed by RT-PCR 4 days after transduction/puromycin selection. Expression values were normalized to *GAPDH* levels and displayed relative to the vector control arbitrarily set as 100. Error bars represent standard deviations of triplicate PCRs.

(E) A three-step model of MLL-dependent transcription.

MLL complexes are normally separate biochemical entities, our studies support a dependent role for the AEP complex in physiologic MLL target gene expression pathways, whose conditional recruitment mechanisms are often bypassed by leukemic MLL fusion proteins.

The AEP complex purified from leukemia cell lines under our experimental conditions contained ENL as an integral component but lacked a number of previously reported ENL-associated proteins, most notably the DOT1L histone methyltransferase (Mueller et al., 2007). Our domain-mapping analyses provide a molecular basis for its absence in that DOT1L and AF4 family proteins use the same binding surface within the AHD of ENL. Because of this physical constraint, DOT1L and AF4 family proteins are incapable of simultaneously associating with the

AHD to form an AF4/ENL/DOT1L trimeric complex. Therefore, retention of DOT1L in the AF4 complex previously identified in thymus homogenates (Bitoun et al., 2007) is likely mediated by other proteins (e.g., AF10 and RNAPII) but not by ENL/AF9. Our data suggest that an endogenous ENL/DOT1L complex and AEP normally exist as separate entities consistent with previous suggestions that ENL may participate in a mixture of different subcomplexes (Mueller et al., 2007).

A role for ENL in multiple subcomplexes raises the issue of which of its molecular interactions is essential for MLL leukemogenesis. This issue was addressed by assessing the oncogenic potential of MLL fused with the DOT1L catalytic domain, which effectively bypasses ENL. Contrary to a previous report (Okada et al., 2005), MLL-DOT1L was not sufficient for transactivation of MLL target genes and transformation of myeloid progenitors under our experimental conditions that read out the oncogenic properties of MLL-AF5q31 and MLL-ENL. This finding indicates that aberrant recruitment of AEP, not DOT1L, plays a primary rate-limiting role in transactivation and transformation by MLL fusion proteins, a conclusion further supported by structure/function analysis of MLL-AF5q31 showing that its CHD, which mediates hetero-interactions with AF4 family members, was necessary and sufficient for transformation.

Nevertheless, ChIP analyses by us and others show that H3K79 methylation marks are present at most MLL-AF4-target loci (Figure 2B) (Krivtsov et al., 2008; Guenther et al., 2008), indicating that there is a strong functional interconnection between AEP and DOT1L. DOT1L-dependent H3K79 methylation is associated with transcribed regions and stimulated by histone H2B K120 mono-ubiquitination (a histone mark accompanied with transcription), but is not required for transcription itself (Steger et al., 2008; McGinty et al., 2008). This finding suggests that DOT1L-dependent H3K79 methylation occurs after the traverse of RNAPII and may play roles in the maintenance of transcriptional memory rather than initiating transcription per se. In this context, our studies support dual roles for ENL, which is capable of interacting with AEP or DOT1L through its AHD to sequentially recruit them to the same target chromatin, possibly via its N-terminal YEATS domain that retains a chromatin binding property (Zeisig et al., 2005).

Our data demonstrate that AEP colocalizes with WT MLL on target promoters indicative of a role in physiologic as well as oncogenic MLL-dependent transcriptional pathways. Supporting this notion, knockdown of *ENL* impaired expression of MLL target genes in MEFs and U937 cells (Figures 8B and 8D), and *Af9*-deficient mice display homeotic transformations similar to those of *Mll*-deficient mice (Collins et al., 2002). The recruitment of AEP to MLL-target loci appears to be nonconstitutive because some MLL-occupied loci do not contain AEP (Figure 6B). Because the presence of the MLL complex does not invariably correlate with occupancy by AEP, other factors or signals yet to be identified are likely required for AEP recruitment. On the basis of these observations and speculations, we propose a three-step model in which WT MLL first establishes/maintains the transcriptionally poised state (Step 1), AEP is then recruited to facilitate onset of transcriptional initiation and/or elongation (Step 2), which is followed by DOT1L-dependent H3K79 methylation post-transcription (Step 3) (Figure 8E). In this model, ENL serves a key role in sequential recruitment of AEP and DOT1L, respectively.

To date, up to 50 different proteins have been reported to fuse with *MLL* in human leukemias. This promiscuity poses a question as to whether any common trait is shared among the fusion partners. We demonstrate here that AEP recruitment is a downstream event in physiologic MLL-dependent transcriptional pathways and is regulated in a context-dependent manner. MLL-AF4 and MLL-ENL family fusions transform myeloid progenitors by constitutively recruiting AEP to MLL-target loci through direct association. Thus, one of the major mechanisms of MLL-dependent transformation is constitutive activation of MLL-dependent transcription by direct recruitment of AEP, which circumvents the regulatory mechanisms that normally control AEP recruitment (Figure 8E).

AEP does not physically interact with MLL-AF6, but nevertheless consistently colocalizes with MLL-AF6 at target chromatin to activate transcription (Figures 6A and 8E). Although the mechanism of this aberrant AEP recruitment is unknown, it indicates that AEP serves an even broader role in MLL leukemogenesis beyond the subset of fusions with AEP components. Determination of whether this role may extend to other MLL fusion proteins requires further investigation. Nevertheless, our studies show that most of the frequently occurring MLL fusions (e.g., MLL-AF4, MLL-AF9, MLL-ENL, and MLL-AF6) use a similar strategy for leukemic transformation, in which AEP is constitutively recruited to MLL target genes either directly or indirectly.

A critical role for AEP in MLL-mediated leukemic transformation suggests that it may be an ideal target for molecular therapy of MLL-associated leukemias. In this regard, our results tentatively support the rationale for CDK9 inhibition as a potential therapeutic strategy, or inhibition of DOT1L whose activity appears to be functionally linked to AEP and possibly plays important roles in the maintenance of the epigenetic status of target genes. However, these molecules are likely to have more generalized roles other than AEP-dependent transcription (Jones et al., 2008; Peterlin and Price, 2006); therefore, serious side effects might occur if they are effectively inhibited. Thus, compounds that specifically target the function of AF4- and ENL family proteins but not P-TEFb or DOT1L may selectively inhibit MLL-dependent transcription and benefit the treatment of MLL-associated leukemias.

EXPERIMENTAL PROCEDURES

Monoclonal Antibodies

Highly specific monoclonal antibodies were generated against MBP fusion proteins containing portions of human AF4 (aa 782–979) (clone 2C.1), human AF5q31 (aa 489–680) (clone 1.3), and human ENL (414–472) (clone 3.1), respectively.

Cell Culture

Human leukemia cell lines K562, HB1119, SEM-K2, KP-L-RY, ML-2, MV4-11, and U937 were cultured in RPMI 1640 medium supplemented with 15% fetal calf serum and nonessential amino acids. MEFs were prepared from E11.5 p53 null embryos. The 293T and plat-E cell lines and MEFs were cultured in Dulbecco's modified Eagle's medium (DMEM) supplemented with 15% fetal calf serum and nonessential amino acids.

Purification of the AEP Complex, Immunoprecipitation, and Western Blotting

The purification procedure for AEP is described in the Supplemental Experimental Procedures. Immunoprecipitation and western blotting methods

are described elsewhere (Yokoyama et al., 2004; 2005). Primary antibodies used in this study are summarized in the Supplemental Experimental Procedures.

Quantitative RT-PCR

Reverse transcription and quantitative PCR were performed as described elsewhere (Yokoyama et al., 2005; Yokoyama and Cleary, 2008) using Taqman probes purchased from Applied Biosystems. The details of the probe set are summarized in the Supplemental Experimental Procedures. Expression levels (average values and standard deviations of triplicate determinations) normalized to housekeeping genes such as *GAPDH* and *β-ACTIN* were calculated using a standard curve and the relative quantification method as described in ABI User Bulletin #2.

Chromatin Immunoprecipitation Assay

Chromatin immunoprecipitations were performed as described elsewhere (Weinmann and Farnham, 2002; Yokoyama and Cleary, 2008). Primary antibodies used in ChIP assays are summarized in Supplemental Experimental Procedures. Quantitative PCR was performed on the precipitated DNAs in triplicate using primers and probes described in Supplemental Experimental Procedures. The values relative to input were determined using a standard curve and the relative quantification method as described in ABI User Bulletin #2.

Vector Construction

cDNA fragments of AF4 and AF5q31 were cloned into pcDNA3.1/*myc*-His A (Invitrogen) for expressing c-*myc* tagged proteins, or pBICEP-CMV-2 (Sigma) for expressing FLAG-tagged proteins. pMSCV-neo constructs encoding MLL-ENL, MLL-AF9, and MLL-AF6 were described elsewhere (Ayton and Cleary, 2003; Somervaille and Cleary, 2006). pMSCV-hygro-Xpress tagged ENL and pMSCV-neo-Xpress tagged MLL-AF5q31-34 were generated by fusing the Xpress-tag sequence from pcDNA4 HisMax vector with the cDNAs of ENL or MLL-AF5q31, respectively. Other expression vectors for various MLL mutants were generated by restriction enzyme digestion or PCR-based mutagenesis. Various FLAG-tagged MLL fusions were also cloned into pCMV5 vector and used for IP analysis. The expression vectors for FLAG-tagged GAL4 fusion proteins were constructed by PCR using pM (Clontech) as template and cloned into pCMV5 vector. The sh-RNA expression vectors targeting murine *Enl* (TRCN0000084405) and human *ENL* (TRCN000019291[#1], TRCN000019293[#2]) were purchased from Open Biosystems.

Virus Production

Ecotropic retrovirus was produced using plat-E packaging cells (Morita et al., 2000). Lentivirus was produced by cotransfection of 293T cells with viral vectors and pCMV dR8.74 and pMD.G packaging constructs (Dull et al., 1998). Supernatant medium containing virus was harvested 48 hr after transfection and was used for transductions.

Myeloid Progenitor Transformation Assay

Myeloid progenitor transformation was assessed as described elsewhere (Lavau et al., 1997; Yokoyama and Cleary, 2008) using cells harvested from the femurs of CD45.1 inbred C57BL/6 mice. C-kit-positive cells were enriched by immunomagnetic selection using an Auto MACS (Miltenyi Biotech), were transduced with recombinant retrovirus by spinoculation, and were plated in methylcellulose medium (M3231, StemCell Technologies) containing SCF, IL-3, IL-6, and GM-CSF. The colony-forming units (CFUs) per 10^4 plated cells were quantified after 5–7 days of culture and were expressed as the average and standard deviation of at least triplicate determinations. For secondary transductions, 10^5 cells were transduced with retrovirus by spinoculation, were cultured in methylcellulose medium overnight, and were selected for drug resistance (hygromycin 750 μg/ml, puromycin 4 μg/ml) for at least 2 days prior to CFC enumeration.

Transactivation Assay

Transactivation assays were performed using 293T cells as described elsewhere (Yokoyama et al., 2002). Cells cultured in 24-well dishes were transfected with 25 ng of pRL-tk, 250 ng of pFR-luc, and 500 ng of pCMV5 FLAG-GAL4 fusion protein vector per well. Cells were lysed 24 hr later and analyzed for luciferase activity using a dual luciferase assay kit according to the manufacturer's instructions (Promega). Relative luciferase activities were normalized to renilla luciferase activities and expressed with the average values and standard deviations of triplicate determinations relative to the GAL4 DNA binding domain controls.

SUPPLEMENTAL INFORMATION

Supplemental information includes five figures and Supplemental Experimental Procedures and may be found with this article online at doi:10.1016/j.ccr.2009.12.040.

ACKNOWLEDGMENTS

We thank Dr. M. Meyerson for providing *Men1* conditional knockout mice, Dr. T. Kitamura for the plat-E cell line, Dr. K. Yamagata for the DOT1L expression vector, and Dr. Y. Zhang for the MLL-DOT1L expression vector. We thank C. Nicolas, M. Ambrus, B. Rouse, C. Hatanaka and M. Kawaguchi, for technical assistance. A.Y. was supported by a Special Fellow Award from the Leukemia and Lymphoma Society. These studies were supported by the Children's Health Initiative of the Packard Foundation and grants from the National Institutes of Health (CA55029 and CA116606) and in part by Grants-in-Aid for Cancer Research (21-6-1) and for the Third-Term Comprehensive 10-Year Strategy for Cancer Control from the Ministry of Health, Labor of Japan.

Received: September 1, 2009
Revised: November 9, 2009
Accepted: December 4, 2009
Published online: February 11, 2010

REFERENCES

Ayton, P.M., and Cleary, M.L. (2003). Transformation of myeloid progenitors by MLL oncoproteins is dependent on Hoxa7 and Hoxa9. Genes Dev. *17*, 2298–2307.

Ayton, P.M., Chen, E.H., and Cleary, M.L. (2004). Binding to nonmethylated CpG DNA is essential for target recognition, transactivation, and myeloid transformation by an MLL oncoprotein. Mol. Cell. Biol. *24*, 10470–10478.

Bitoun, E., Oliver, P.L., and Davies, K.E. (2007). The mixed-lineage leukemia fusion partner AF4 stimulates RNA polymerase II transcriptional elongation and mediates coordinated chromatin remodeling. Hum. Mol. Genet. *16*, 92–106.

Cheung, N., Chan, L.C., Thompson, A., Cleary, M.L., and So, C.W. (2007). Protein arginine-methyltransferase-dependent oncogenesis. Nat. Cell Biol. *9*, 1208–1215.

Collins, E.C., Appert, A., Ariza-McNaughton, L., Pannell, R., Yamada, Y., and Rabbitts, T.H. (2002). Mouse Af9 is a controller of embryo patterning, like Mll, whose human homologue fuses with Af9 after chromosomal translocation in leukemia. Mol. Cell. Biol. *22*, 7313–7324.

Cozzio, A., Passegue, E., Ayton, P.M., Karsunky, H., Cleary, M.L., and Weissman, I.L. (2003). Similar MLL-associated leukemias arising from self-renewing stem cells and short-lived myeloid progenitors. Genes Dev. *17*, 3029–3035.

Daser, A., and Rabbitts, T.H. (2004). Extending the repertoire of the mixed-lineage leukemia gene MLL in leukemogenesis. Genes Dev. *18*, 965–974.

DiMartino, J.F., Miller, T., Ayton, P.M., Landewe, T., Hess, J.L., Cleary, M.L., and Shilatifard, A. (2000). A carboxy-terminal domain of ELL is required and sufficient for immortalization of myeloid progenitors by MLL-ELL. Blood *96*, 3887–3893.

DiMartino, J.F., Ayton, P.M., Chen, E.H., Naftzger, C.C., Young, B.D., and Cleary, M.L. (2002). The AF10 leucine zipper is required for leukemic transformation of myeloid progenitors by MLL-AF10. Blood *99*, 3780–3785.

Domer, P.H., Fakharzadeh, S.S., Chen, C.S., Jockel, J., Johansen, L., Silverman, G.A., Kersey, J.H., and Korsmeyer, S.J. (1993). Acute mixed-lineage leukemia t(4;11)(q21;q23) generates an MLL-AF4 fusion product. Proc. Natl. Acad. Sci. USA *90*, 7884–7888.

Dreyling, M.H., Martinez-Climent, J.A., Zheng, M., Mao, J., Rowley, J.D., and Bohlander, S.K. (1996). The t(10;11)(p13;q14) in the U937 cell line results in the fusion of the AF10 gene and CALM, encoding a new member of the AP-3 clathrin assembly protein family. Proc. Natl. Acad. Sci. USA *93*, 4804–4809.

Dull, T., Zufferey, R., Kelly, M., Mandel, R.J., Nguyen, M., Trono, D., and Naldini, L. (1998). A third-generation lentivirus vector with a conditional packaging system. J. Virol. *72*, 8463–8471.

Erfurth, F., Hemenway, C.S., de Erkenez, A.C., and Domer, P.H. (2004). MLL fusion partners AF4 and AF9 interact at subnuclear foci. Leukemia *18*, 92–102.

Gilliland, D.G. (2002). Molecular genetics of human leukemias: new insights into therapy. Semin. Hematol. *39*, 6–11.

Guenther, M.G., Jenner, R.G., Chevalier, B., Nakamura, T., Croce, C.M., Canaani, E., and Young, R.A. (2005). Global and Hox-specific roles for the MLL1 methyltransferase. Proc. Natl. Acad. Sci. USA *102*, 8603–8608.

Guenther, M.G., Lawton, L.N., Rozovskaia, T., Frampton, G.M., Levine, S.S., Volkert, T.L., Croce, C.M., Nakamura, T., Canaani, E., and Young, R.A. (2008). Aberrant chromatin at genes encoding stem cell regulators in human mixed-lineage leukemia. Genes Dev. *22*, 3403–3408.

Hughes, C.M., Rozenblatt-Rosen, O., Milne, T.A., Copeland, T.D., Levine, S.S., Lee, J.C., Hayes, D.N., Shanmugam, K.S., Bhattacharjee, A., Biondi, C.A., et al. (2004). Menin associates with a trithorax family histone methyltransferase complex and with the hoxc8 locus. Mol. Cell *13*, 587–597.

Huret, J.L., Dessen, P., and Bernheim, A. (2001). An atlas of chromosomes in hematological malignancies. Example: 11q23 and MLL partners. Leukemia *15*, 987–989.

Iida, S., Seto, M., Yamamoto, K., Komatsu, H., Tojo, A., Asano, S., Kamada, N., Ariyoshi, Y., Takahashi, T., and Ueda, R. (1993). MLLT3 gene on 9p22 involved in t(9;11) leukemia encodes a serine/proline rich protein homologous to MLLT1 on 19p13. Oncogene *8*, 3085–3092.

Jansen, M.W., van der Velden, V.H., and van Dongen, J.J. (2005). Efficient and easy detection of MLL-AF4, MLL-AF9 and MLL-ENL fusion gene transcripts by multiplex real-time quantitative RT-PCR in TaqMan and LightCycler. Leukemia *19*, 2016–2018.

Jones, B., Su, H., Bhat, A., Lei, H., Bajko, J., Hevi, S., Baltus, G.A., Kadam, S., Zhai, H., Valdez, R., et al. (2008). The histone H3K79 methyltransferase Dot1L is essential for mammalian development and heterochromatin structure. PLoS Genet. *4*, e1000190. 10.1371/journal.pgen.1000190.

Krivtsov, A.V., and Armstrong, S.A. (2007). MLL translocations, histone modifications and leukaemia stem-cell development. Nat. Rev. Cancer *7*, 823–833.

Krivtsov, A.V., Feng, Z., Lemieux, M.E., Faber, J., Vempati, S., Sinha, A.U., Xia, X., Jesneck, J., Bracken, A.P., Silverman, L.B., et al. (2008). H3K79 methylation profiles define murine and human MLL-AF4 leukemias. Cancer Cell *14*, 355–368.

Lavau, C., Szilvassy, S.J., Slany, R., and Cleary, M.L. (1997). Immortalization and leukemic transformation of a myelomonocytic precursor by retrovirally transduced HRX-ENL. EMBO J. *16*, 4226–4237.

Lavau, C., Du, C., Thirman, M., and Zeleznik-Le, N. (2000). Chromatin-related properties of CBP fused to MLL generate a myelodysplastic-like syndrome that evolves into myeloid leukemia. EMBO J. *19*, 4655–4664.

Li, B., Carey, M., and Workman, J.L. (2007). The role of chromatin during transcription. Cell *128*, 707–719.

Ma, C., and Staudt, L.M. (1996). LAF-4 encodes a lymphoid nuclear protein with transactivation potential that is homologous to AF-4, the gene fused to MLL in t(4;11) leukemias. Blood *87*, 734–745.

McGinty, R.K., Kim, J., Chatterjee, C., Roeder, R.G., and Muir, T.W. (2008). Chemically ubiquitylated histone H2B stimulates hDot1L-mediated intranucleosomal methylation. Nature *453*, 812–816.

Milne, T.A., Briggs, S.D., Brock, H.W., Martin, M.E., Gibbs, D., Allis, C.D., and Hess, J.L. (2002). MLL targets SET domain methyltransferase activity to Hox gene promoters. Mol. Cell *10*, 1107–1117.

Milne, T.A., Hughes, C.M., Lloyd, R., Yang, Z., Rozenblatt-Rosen, O., Dou, Y., Schnepp, R.W., Krankel, C., Livolsi, V.A., Gibbs, D., et al. (2005). Menin and MLL cooperatively regulate expression of cyclin-dependent kinase inhibitors. Proc. Natl. Acad. Sci. USA *102*, 749–754.

Morita, S., Kojima, T., and Kitamura, T. (2000). Plat-E: an efficient and stable system for transient packaging of retroviruses. Gene Ther. *7*, 1063–1066.

Morrissey, J.J., Raney, S., and Cleary, M.L. (1997). The FEL (AF-4) protein donates transcriptional activation sequences to Hrx-Fel fusion proteins in leukemias containing T(4;11)(Q21;Q23) chromosomal translocations. Leuk. Res. *21*, 911–917.

Mueller, D., Bach, C., Zeisig, D., Garcia-Cuellar, M.P., Monroe, S., Sreekumar, A., Zhou, R., Nesvizhskii, A., Chinnaiyan, A., Hess, J.L., and Slany, R.K. (2007). A role for the MLL fusion partner ENL in transcriptional elongation and chromatin modification. Blood *110*, 4445–4454.

Nakamura, T., Alder, H., Gu, Y., Prasad, R., Canaani, O., Kamada, N., Gale, R.P., Lange, B., Crist, W.M., Nowell, P.C., et al. (1993). Genes on chromosomes 4, 9, and 19 involved in 11q23 abnormalities in acute leukemia share sequence homology and/or common motifs. Proc. Natl. Acad. Sci. USA *90*, 4631–4635.

Nakamura, T., Largaespada, D.A., Shaughnessy, J.D., Jr., Jenkins, N.A., and Copeland, N.G. (1996). Cooperative activation of Hoxa and Pbx1-related genes in murine myeloid leukaemias. Nat. Genet. *12*, 149–153.

Nilson, I., Reichel, M., Ennas, M.G., Greim, R., Knorr, C., Siegler, G., Greil, J., Fey, G.H., and Marschalek, R. (1997). Exon/intron structure of the human AF-4 gene, a member of the AF-4/LAF-4/FMR-2 gene family coding for a nuclear protein with structural alterations in acute leukaemia. Br. J. Haematol. *98*, 157–169.

Okada, Y., Feng, Q., Lin, Y., Jiang, Q., Li, Y., Coffield, V.M., Su, L., Xu, G., and Zhang, Y. (2005). hDOT1L links histone methylation to leukemogenesis. Cell *121*, 167–178.

Peterlin, B.M., and Price, D.H. (2006). Controlling the elongation phase of transcription with P-TEFb. Mol. Cell *23*, 297–305.

Prasad, R., Yano, T., Sorio, C., Nakamura, T., Rallapalli, R., Gu, Y., Leshkowitz, D., Croce, C.M., and Canaani, E. (1995). Domains with transcriptional regulatory activity within the ALL1 and AF4 proteins involved in acute leukemia. Proc. Natl. Acad. Sci. USA *92*, 12160–12164.

Pui, C.H., Relling, M.V., and Downing, J.R. (2004). Acute lymphoblastic leukemia. N. Engl. J. Med. *350*, 1535–1548.

Saunders, A., Core, L.J., and Lis, J.T. (2006). Breaking barriers to transcription elongation. Nat. Rev. Mol. Cell Biol. *7*, 557–567.

Slany, R.K., Lavau, C., and Cleary, M.L. (1998). The oncogenic capacity of HRX-ENL requires the transcriptional transactivation activity of ENL and the DNA binding motifs of HRX. Mol. Cell. Biol. *18*, 122–129.

So, C.W., and Cleary, M.L. (2002). MLL-AFX requires the transcriptional effector domains of AFX to transform myeloid progenitors and transdominantly interfere with forkhead protein function. Mol. Cell. Biol. *22*, 6542–6552.

So, C.W., and Cleary, M.L. (2003). Common mechanism for oncogenic activation of MLL by forkhead family proteins. Blood *101*, 633–639.

Somervaille, T.C., and Cleary, M.L. (2006). Identification and characterization of leukemia stem cells in murine MLL-AF9 acute myeloid leukemia. Cancer Cell *10*, 257–268.

Srinivasan, R.S., Nesbit, J.B., Marrero, L., Erfurth, F., LaRussa, V.F., and Hemenway, C.S. (2004). The synthetic peptide PFWT disrupts AF4-AF9 protein complexes and induces apoptosis in t(4;11) leukemia cells. Leukemia *18*, 1364–1372.

Steger, D.J., Lefterova, M.I., Ying, L., Stonestrom, A.J., Schupp, M., Zhuo, D., Vakoc, A.L., Kim, J.E., Chen, J., Lazar, M.A., et al. (2008). DOT1L/KMT4 recruitment and H3K79 methylation are ubiquitously coupled with gene transcription in mammalian cells. Mol. Cell. Biol. *28*, 2825–2839.

Taki, T., Kano, H., Taniwaki, M., Sako, M., Yanagisawa, M., and Hayashi, Y. (1999). AF5q31, a newly identified AF4-related gene, is fused to MLL in infant acute lymphoblastic leukemia with ins(5;11)(q31;q13q23). Proc. Natl. Acad. Sci. USA *96*, 14535–14540.

Tkachuk, D.C., Kohler, S., and Cleary, M.L. (1992). Involvement of a homolog of *Drosophila* trithorax by 11q23 chromosomal translocations in acute leukemias. Cell *71*, 691–700.

von Bergh, A.R., Beverloo, H.B., Rombout, P., van Wering, E.R., van Weel, M.H., Beverstock, G.C., Kluin, P.M., Slater, R.M., and Schuuring, E. (2002).

LAF4, an AF4-related gene, is fused to MLL in infant acute lymphoblastic leukemia. Genes Chromosomes Cancer *35*, 92–96.

Weinmann, A.S., and Farnham, P.J. (2002). Identification of unknown target genes of human transcription factors using chromatin immunoprecipitation. Methods *26*, 37–47.

Wong, P., Iwasaki, M., Somervaille, T.C., So, C.W., and Cleary, M.L. (2007). Meis1 is an essential and rate-limiting regulator of MLL leukemia stem cell potential. Genes Dev. *21*, 2762–2774.

Yokoyama, A., and Cleary, M.L. (2008). Menin critically links MLL proteins with LEDGF on cancer-associated target genes. Cancer Cell *14*, 36–46.

Yokoyama, A., Kitabayashi, I., Ayton, P.M., Cleary, M.L., and Ohki, M. (2002). Leukemia proto-oncoprotein MLL is proteolytically processed into 2 fragments with opposite transcriptional properties. Blood *100*, 3710–3718.

Yokoyama, A., Wang, Z., Wysocka, J., Sanyal, M., Aufiero, D.J., Kitabayashi, I., Herr, W., and Cleary, M.L. (2004). Leukemia proto-oncoprotein MLL forms a SET1-like histone methyltransferase complex with menin to regulate Hox gene expression. Mol. Cell. Biol. *24*, 5639–5649.

Yokoyama, A., Somervaille, T.C., Smith, K.S., Rozenblatt-Rosen, O., Meyerson, M., and Cleary, M.L. (2005). The menin tumor suppressor protein is an essential oncogenic cofactor for MLL-associated leukemogenesis. Cell *123*, 207–218.

Zeisig, D.T., Bittner, C.B., Zeisig, B.B., Garcia-Cuellar, M.P., Hess, J.L., and Slany, R.K. (2005). The eleven-nineteen-leukemia protein ENL connects nuclear MLL fusion partners with chromatin. Oncogene *24*, 5525–5532.

Zhang, W., Xia, X., Reisenauer, M.R., Hemenway, C.S., and Kone, B.C. (2006). Dot1a-AF9 complex mediates histone H3 Lys-79 hypermethylation and repression of ENaCalpha in an aldosterone-sensitive manner. J. Biol. Chem. *281*, 18059–18068.

Journal of Gastroenterology and Hepatology

JGHF

doi:10.1111/j.1440-1746.2011.06723.x

MECHANISMS OF GASTROINTESTINAL, PANCREATIC AND LIVER DISEASES

Molecular mechanisms of hepatocarcinogenesis in chronic hepatitis C virus infection

Taro Yamashita, Masao Honda and Shuichi Kaneko

Department of Gastroenterology, Kanazawa University Graduate School of Medical Science, Kanazawa, Ishikawa, Japan

Key words
hepatitis C virus, hepatocellular carcinoma, transcriptome.

Accepted for publication 10 March 2011.

Correspondence
Professor Shuichi Kaneko, Department of Gastroenterology, Kanazawa University Graduate School of Medical Science, 13-1 Takara-Machi, Kanazawa, Ishikawa 920-8641, Japan. Email: skaneko@m-kanazawa.jp

Abstract

Hepatitis C virus (HCV) infection is a major cause of hepatocellular carcinoma (HCC) and chronic liver disease worldwide. Recent developments and advances in HCV replication systems *in vitro* and *in vivo*, transgenic animal models, and gene expression profiling approaches have provided novel insights into the mechanisms of HCV replication. They have also helped elucidate host cellular responses, including activated/inactivated signaling pathways, and the relationship between innate immune responses by HCV infection and host genetic traits. However, the mechanisms of hepatocyte malignant transformation induced by HCV infection are still largely unclear, most likely due to the heterogeneity of molecular paths leading to HCC development in each individual. In this review, we summarize recent advances in knowledge about the mechanisms of hepatocarcinogenesis induced by HCV infection.

Introduction

Hepatocellular carcinoma (HCC) is the fifth most common malignancy and the third leading cause of cancer death worldwide.[1] The majority of HCCs arise from a background of chronic liver diseases caused by infection with hepatitis B virus (HBV) or hepatitis C virus (HCV).[2] Although both viruses are hepatotropic and regarded as causative agents of HCC, the underlying mechanisms of hepatocarcinogenesis are considered to be largely different, partly due to differences in the nature of DNA viruses (with an integration capacity for the host genome) and RNA viruses (with no genome integration capacity).

Hepatitis C virus is an RNA virus that is unable to integrate into the host genome but, instead, its proteins interact with various host proteins and induce host responses that potentially contribute to the malignant transformation of cells. In addition, HCC usually develops in the setting of liver cirrhosis after long-term continuous inflammation/regeneration processes; these accelerate the turnover of hepatocytes with increased risk of replication errors and DNA damage. Furthermore, recent genome-wide association studies have suggested that the natural course of HCV infection might be modified by the genetic background of the host.[3,4] Thus, both host and virus factors are considered to affect the process of hepatocarcinogenesis in a complex manner.

In this review, we summarize the current knowledge of the mechanisms of hepatocarcinogenesis induced by HCV infection. We also focus on recent findings of transcriptomic characteristics of HCV-related HCC and summarize the potential signaling pathways that are altered in this condition.

Epidemiology

Chronic HCV infection is a major risk factor for the development of HCC worldwide. According to the World Health Organization (WHO), approximately 170 million people are chronically infected with HCV. Although epidemiological evidence has suggested a clear, close relationship between HCV infection and HCC,[5,6] the prevalence of HCV infection in HCC patients differs noticeably between geographical regions. Thus, HCV infection is found in 70–80% of HCC patients in Japan, 70% in Egypt, 40–50% in Italy and Spain, about 20% in the United States (US), and less than 10% in China.[7–9] In industrialized countries including the US, a recent increase in HCC incidence and mortality has been observed, potentially due to the rising incidence of HCV infection transmitted through contaminated blood.[10]

Hepatitis C virus increases the risk of HCC by promoting inflammation and fibrosis of the infected liver that eventually results in liver cirrhosis. Once HCV-related cirrhosis is established, HCC develops at an annual rate of about 4–7%.[11] Other factors including alcohol intake, diabetes, and obesity have also been reported to increase the risk of HCC development by about two- to fourfold, indicating a strong life-style effect on the process of hepatocarcinogenesis.[12,13] Age and male gender are also contributing risk factors for HCV-related HCC, although the detailed mechanisms are still debatable.

Virus proteins and host responses

Hepatitis C virus belongs to the Flaviviridae family. It has a positive-stranded linear RNA genome of about 9.6-kb containing a

single large open reading frame encoding three structural (core, E1, and E2) and seven non-structural (p7, NS2, NS3, NS4A, NS4B, NS5A, and NS5B) proteins.[14] The structural proteins form the HCV virions, whereas non-structural proteins are involved in the processes of viral replication, assembly, and maturation. HCV proteins are known to be processed by host and viral proteases. Both structural and non-structural proteins can interact with various host cellular proteins to potentially promote the malignant transformation of hepatocytes (see recent reviews[7,15,16]). In this review, because of space limitations, we focus on the findings of core and NS5A proteins in terms of host responses potentially evoked during the process of HCV-related hepatocarcinogenesis.

Core protein

Hepatitis C virus core is a 21-kDa nucleocapsid protein with an RNA-binding capacity. In addition to its function in regulating HCV-RNA translation and HCV particle assembly, core protein is known to be involved in mediating the alteration of various host cell signaling pathways, transcriptional activation, modulation of immune responses, apoptosis, oxidative stress, and lipid metabolism.[7] Several recent studies have indicated the statistically significant high frequency of mutations in the *core* gene in HCV-infected patients who developed HCC.[17,18] However, the functional relevance of mutant core proteins on the malignant transformation of hepatocytes or the HCV life cycle has yet to be clarified.

Evidence of core protein as a causative agent of HCC was initially obtained from the transgenic mice model in which *core* gene overexpression, under the regulation of the HBV regulatory element used as a promoter, resulted in steatosis of mouse livers in early life, with subsequent development of adenoma and HCC.[19] However, another mouse model using a different promoter and of a different strain background resulted only in steatosis or different phenotypes without HCC development.[20,21] Similar controversial findings were reported in transgenic mice expressing HCV polyprotein or structural protein with regards to the development of HCC.[22,23] Thus, the role of core protein alone in the development of HCC remains unclear in transgenic mouse models.

Although the direct role of core protein in the malignant transformation of hepatocytes is still under investigation, it seems to be related to the development of hepatic steatosis.[19,24] Indeed, steatosis is one of the risk factors for the development of HCV-related HCC,[25,26] and activation of the lipogenic pathway has been reported in a subset of HCC cases.[27] Core protein is associated with the surface of lipid droplets in infected cells and might be directly related to steatosis through several factors responsible for lipid biogenesis and degradation, including peroxisome proliferator-activated receptor alpha and sterol-regulatory element binding protein-1.[21,28–30] Furthermore, core protein is reported to interact with endoplasmic reticulum (ER) or mitochondrial outer membranes and induce ER stress by perturbation of protein folding or by the accumulation of reactive oxygen species (ROS) through mitochondrial dysfunction.[31,32] ROS produced in this way might result in DNA damage to the host genome and accelerate the process of hepatocarcinogenesis. Increased hepatic iron deposition may also induce oxidative stress and lipid peroxidation, thus increasing the risk of HCC development in HCV polyprotein transgenic mice.[33]

Since the discovery of HCV, various studies have investigated the role of core on host cells. Its effects have been demonstrated on signaling pathways responsible for the cell cycle, and apoptosis through interaction with several tumor suppressors including p53, p73, and p21[34–39] as well as apoptosis regulators such as tumor necrosis factor-α (TNF-α) signaling or Bcl-2 members.[40–42] However, the data obtained from these studies are relatively inconsistent with each other and have varied across experimental models. Core protein may influence the growth and proliferation of host cells through activation of signaling pathways such as Raf/mitogen activated protein kinase (MAPK),[43] Wnt/beta catenin,[16] and transforming growth factor-β (TGF-β).[15,44] These pathways are known to be activated in HCC.[45] The findings therefore indicate a potential role for core in cell proliferation or suppression of apoptosis during malignant transformation of hepatocytes in the liver of chronic hepatitis C, where chronic inflammation and regeneration of hepatocytes continuously occurs.

NS5A protein

NS5A is a 56–58-kDa protein phosphorylated at serine residues by serine-threonine kinase[46] and is essential for replication of the HCV genome. NS5A protein forms part of the viral replicase complex and is localized mainly in the cytoplasm of infected cells in association with the ER. NS5A can become a lower molecular weight protein through post-translational modification, after which it can undergo translocation to the nucleus where it acts as a transcriptional activator. High frequencies of wild-type *NS5A* genes were reported to be dominant in liver cirrhosis patients who finally developed HCC compared with those who did not,[47] but the mechanistic significance of the *NS5A* wild/mutant genotypes in the process of HCV-related hepatocarcinogenesis remains uncertain.

NS5A protein has been suggested to interact with various signaling pathways including cell cycle/apoptosis[48] and lipid metabolism[28,49,50] in host cells and shares some signaling targets with core protein. NS5A is recognized as a transcriptional activator for many target genes[51] including p53 and its binding protein, TATA binding protein (TBP). Transcription factor IID activities were reported to be modified by NS5A in the suppression of p53-dependent transcriptional transactivation and apoptosis.[52,53] NS5A may also interact with pathways such as Bcl2,[54] phosphatidylinositol 3-kinase (PI3-K),[55] Wnt/beta catenin signaling,[56] and mTOR[57] to activate cell proliferation signaling and inhibit apoptosis.

Taken together, intriguing data concerning the function of core and NS5A proteins on host cell signaling pathways, transcriptional activation, apoptosis, oxidative stress, and lipid metabolism described above suggest a diverse role for HCV proteins in the pathophysiology of chronic hepatitis C that leads to malignant transformation in infected hepatocytes. Key findings and present concepts are summarized in Figure 1.

Transcriptomic characteristics of HCV-related HCC

As described above, HCV proteins can evoke various host responses in infected cells at transcriptional/translational/post-translational levels. Furthermore, enhanced cell death/regeneration processes are considered to induce DNA damage and accelerate replication errors that cause frequent mutations and genomic alter-

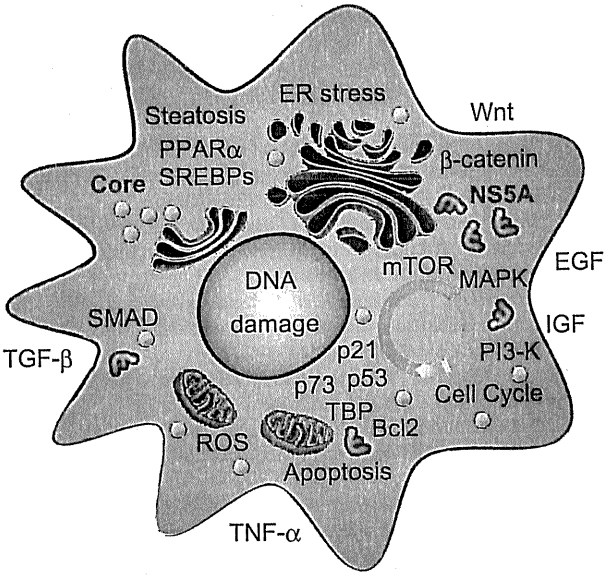

Figure 1 Signaling pathways potentially affected by hepatitis C virus (HCV) proteins. EGF, epidermal growth factor; ER, endoplasmic reticulum; IGF, insulin-like growth factor; MAPK, mitogen activated protein kinase; mTOR, mammalian target of rapamycin; PI3-K, phosphatidylinositol 3-kinase; PPAR, peroxisome proliferator-activated receptor; ROS, reactive oxygen species; SREBP, sterol-regulatory element binding protein; TBP, TATA binding protein.

ation in the host genome. The central dogma is defined as the flow of genetic information from DNA to mRNA and then to protein, so genetic/genomic alterations and transcriptional/translational modifications are ultimately considered to affect the cellular signaling pathway at the transcriptional level.

Over the past decade, several methods (including differential display, serial analysis of gene expression [SAGE], and microarray) have been developed to allow comparative studies of gene expression between normal and cancer cells on a genome-wide scale,[58] and the analysis of a set of all RNA molecules (mainly indicating mRNAs) is termed as whole transcriptome analysis. Extensive transcriptome analysis of HCC and corresponding noncancerous livers has been performed, and the results have greatly increased our knowledge about the transcriptome characteristics of HCV-related HCC.

Early microarray and SAGE studies investigating the gene expression patterns of chronic hepatitis B and C tissues indicated that these two chronic hepatitis tissues had distinct gene expression profiles; the genes activated in chronic hepatitis C were correlated with signaling pathways associated with apoptosis, oxidative stress responses, and Th1 cytokine signaling.[59,60] An early study comparing genes activated in HCV-related and HBV-related HCCs showed that the genes associated with xenobiotic metabolism were more abundantly expressed in HCV-related HCC,[61] suggesting a detoxification role, which is potentially induced by chronic inflammation and generation of ROS resulting from HCV infection. In contrast, HBV-related HCC might closely correlate with the activation of imprint genes, including insulin-like growth factor-II (IGF-II) as investigated by oligo-DNA microarray,[62] suggesting a role of de-differentiation or epigenetic alteration of the host genome in HBV-related HCC. Activation of genes associated with interferon, oxidative stress, apoptosis, and lipid metabolism signaling was detected in HCV-related HCC and chronic hepatitis C specimens,[27,60,63] consistent with numerous functional studies that have investigated the host response evoked by HCV structural and non-structural proteins.[48]

Transcriptome analysis has also recently shed new light on the transcriptional alteration events occurring in early stages of HCV-related hepatocarcinogenesis. *GPC3* (encoding Glypican 3) was identified as one of the most activated transcripts in the early stage of hepatocarcinogenesis,[60,64] while several recent studies showed that gene signatures including *GPC3* can successfully discriminate HCCs from pre-malignant dysplastic nodules and cirrhosis nodules.[65,66] Close examination of genes differentially expressed among cirrhotic nodules, dysplastic nodules, and early and advanced HCV-related HCC tissues has also suggested roles for Toll-like receptor signaling, Wnt signaling, bone morphogenetic protein (BMP)/TGF-β signaling, JAK-STAT signaling, and DNA repair/cell cycle responses in each step of the malignant transformation processes.[67] These processes might therefore provide candidate molecular targets for the chemoprevention of HCV-related HCC.

Recent advances in transcriptome analysis have also provided detailed information on the status of small noncoding RNAs, microRNAs, that can regulate the expression of target genes and viral replication in normal and cancer tissues. Expression of microRNAs including miR-122 and –199a has been reported to modulate HCV replication,[68–70] and miR-122 expression can be regulated by host interferon signaling and responses.[71] HCV protein expression in turn could induce miRNAs and might affect the tumor suppressor DLC1 and the chemosensitivity of malignantly transformed cells.[72,73] Several microRNAs were also differentially expressed between HCV-related and HBV-related HCCs as well as their corresponding non-cancerous liver tissues. The candidate signaling pathways potentially altered by microRNAs in HCV-related tissues were those associated with antigen presentation, cell cycle, and lipid metabolism,[74] consistent with the mRNA microarray data described above. MicroRNAs have also recently been reported to successfully discriminate between HCC and cirrhotic liver tissues,[75] implicating their role in the early stages of malignant transformation. These data suggest that microRNAs may be good targets for the eradication of HCC as well as hepatocytes infected with HCV.

Conclusion

The heterogeneity of genetic/transcriptomic/proteomic events observed in hepatocytes or cell lines expressing HCV proteins and HCV-related HCCs reported thus far has suggested that complex mechanisms underlie malignant transformation induced by HCV infection. These potentially act through convoluted virus-host interactions including HCV replication with host cell cycles, apoptosis, proliferation, quality control of protein synthesis, lipid metabolism, and DNA damage responses. Indeed, HCC is a heterogeneous disease in terms of drug sensitivity, metastatic capacity, and clinical outcome. The heterogeneity of HCV-related HCC may closely correlate with the origin of malignantly transformed cells where multifaceted cellular reactions including apoptosis and

cell proliferation are induced by HCV infection. An in-depth understanding of these molecular complexities associated with HCV-related HCC may provide the opportunity for effective chemoprevention of HCC among those with HCV-cirrhosis, and to design tailor-made treatment options for HCV-related HCC patients in the future.

References

1 Parkin DM, Bray F, Ferlay J, Pisani P. Global cancer statistics, 2002. *CA Cancer J. Clin.* 2005; **55**: 74–108.
2 Yang JD, Roberts LR. Hepatocellular carcinoma: a global view. *Nat. Rev. Gastroenterol. Hepatol.* 2010; **7**: 448–58.
3 Thomas DL, Thio CL, Martin MP *et al.* Genetic variation in IL28B and spontaneous clearance of hepatitis C virus. *Nature* 2009; **461**: 798–801.
4 Tillmann HL, Thompson AJ, Patel K *et al.* A polymorphism near IL28B is associated with spontaneous clearance of acute hepatitis C virus and jaundice. *Gastroenterology* 2010; **139**: 1586–92. 92 e1.
5 Bruix J, Barrera JM, Calvet X *et al.* Prevalence of antibodies to hepatitis C virus in Spanish patients with hepatocellular carcinoma and hepatic cirrhosis. *Lancet* 1989; **2**: 1004–6.
6 Colombo M, Kuo G, Choo QL *et al.* Prevalence of antibodies to hepatitis C virus in Italian patients with hepatocellular carcinoma. *Lancet* 1989; **2**: 1006–8.
7 Liang TJ, Heller T. Pathogenesis of hepatitis C-associated hepatocellular carcinoma. *Gastroenterology* 2004; **127**: S62–71.
8 Yoshizawa H. Hepatocellular carcinoma associated with hepatitis C virus infection in Japan: projection to other countries in the foreseeable future. *Oncology* 2002; **62** (Suppl. 1): 8–17.
9 Yuen MF, Hou JL, Chutaputti A. Hepatocellular carcinoma in the Asia pacific region. *J. Gastroenterol. Hepatol.* 2009; **24**: 346–53.
10 El-Serag HB, Rudolph KL. Hepatocellular carcinoma: epidemiology and molecular carcinogenesis. *Gastroenterology* 2007; **132**: 2557–76.
11 Fattovich G, Stroffolini T, Zagni I, Donato F. Hepatocellular carcinoma in cirrhosis: incidence and risk factors. *Gastroenterology* 2004; **127**: S35–50.
12 Yu MC, Yuan JM. Environmental factors and risk for hepatocellular carcinoma. *Gastroenterology* 2004; **127**: S72–8.
13 Kawaguchi T, Sata M. Importance of hepatitis C virus-associated insulin resistance: therapeutic strategies for insulin sensitization. *World J. Gastroenterol.* 2010; **16**: 1943–52.
14 Penin F, Dubuisson J, Rey FA, Moradpour D, Pawlotsky JM. Structural biology of hepatitis C virus. *Hepatology* 2004; **39**: 5–19.
15 Tsai WL, Chung RT. Viral hepatocarcinogenesis. *Oncogene* 2010; **29**: 2309–24.
16 Levrero M. Viral hepatitis and liver cancer: the case of hepatitis C. *Oncogene* 2006; **25**: 3834–47.
17 Akuta N, Suzuki F, Kawamura Y *et al.* Amino acid substitutions in the hepatitis C virus core region are the important predictor of hepatocarcinogenesis. *Hepatology* 2007; **46**: 1357–64.
18 Fishman SL, Factor SH, Balestrieri C *et al.* Mutations in the hepatitis C virus core gene are associated with advanced liver disease and hepatocellular carcinoma. *Clin. Cancer Res.* 2009; **15**: 3205–13.
19 Moriya K, Fujie H, Shintani Y *et al.* The core protein of hepatitis C virus induces hepatocellular carcinoma in transgenic mice. *Nat. Med.* 1998; **4**: 1065–7.
20 Okuda M, Li K, Beard MR *et al.* Mitochondrial injury, oxidative stress, and antioxidant gene expression are induced by hepatitis C virus core protein. *Gastroenterology* 2002; **122**: 366–75.
21 Perlemuter G, Sabile A, Letteron P *et al.* Hepatitis C virus core protein inhibits microsomal triglyceride transfer protein activity and very low density lipoprotein secretion: a model of viral-related steatosis. *FASEB J.* 2002; **16**: 185–94.
22 Kawamura T, Furusaka A, Koziel MJ *et al.* Transgenic expression of hepatitis C virus structural proteins in the mouse. *Hepatology* 1997; **25**: 1014–21.
23 Wakita T, Taya C, Katsume A *et al.* Efficient conditional transgene expression in hepatitis C virus cDNA transgenic mice mediated by the Cre/loxP system. *J. Biol. Chem.* 1998; **273**: 9001–6.
24 Lerat H, Kammoun HL, Hainault I *et al.* Hepatitis C virus proteins induce lipogenesis and defective triglyceride secretion in transgenic mice. *J. Biol. Chem.* 2009; **284**: 33466–74.
25 Ohata K, Hamasaki K, Toriyama K *et al.* Hepatic steatosis is a risk factor for hepatocellular carcinoma in patients with chronic hepatitis C virus infection. *Cancer* 2003; **97**: 3036–43.
26 Kurosaki M, Hosokawa T, Matsunaga K *et al.* Hepatic steatosis in chronic hepatitis C is a significant risk factor for developing hepatocellular carcinoma independent of age, sex, obesity, fibrosis stage and response to interferon therapy. *Hepatol. Res.* 2010; **40**: 870–7.
27 Yamashita T, Honda M, Takatori H *et al.* Activation of lipogenic pathway correlates with cell proliferation and poor prognosis in hepatocellular carcinoma. *J. Hepatol.* 2009; **50**: 100–10.
28 Dharancy S, Malapel M, Perlemuter G *et al.* Impaired expression of the peroxisome proliferator-activated receptor alpha during hepatitis C virus infection. *Gastroenterology* 2005; **128**: 334–42.
29 Waris G, Felmlee DJ, Negro F, Siddiqui A. Hepatitis C virus induces proteolytic cleavage of sterol regulatory element binding proteins and stimulates their phosphorylation via oxidative stress. *J. Virol.* 2007; **81**: 8122–30.
30 Tanaka N, Moriya K, Kiyosawa K, Koike K, Gonzalez FJ, Aoyama T. PPARalpha activation is essential for HCV core protein-induced hepatic steatosis and hepatocellular carcinoma in mice. *J. Clin. Invest.* 2008; **118**: 683–94.
31 Korenaga M, Wang T, Li Y *et al.* Hepatitis C virus core protein inhibits mitochondrial electron transport and increases reactive oxygen species (ROS) production. *J. Biol. Chem.* 2005; **280**: 37481–8.
32 Li Y, Boehning DF, Qian T, Popov VL, Weinman SA. Hepatitis C virus core protein increases mitochondrial ROS production by stimulation of Ca^{2+} uniporter activity. *FASEB J.* 2007; **21**: 2474–85.
33 Furutani T, Hino K, Okuda M *et al.* Hepatic iron overload induces hepatocellular carcinoma in transgenic mice expressing the hepatitis C virus polyprotein. *Gastroenterology* 2006; **130**: 2087–98.
34 Alisi A, Giambartolomei S, Cupelli F *et al.* Physical and functional interaction between HCV core protein and the different p73 isoforms. *Oncogene* 2003; **22**: 2573–80.
35 Honda M, Kaneko S, Shimazaki T *et al.* Hepatitis C virus core protein induces apoptosis and impairs cell-cycle regulation in stably transformed Chinese hamster ovary cells. *Hepatology* 2000; **31**: 1351–9.
36 Kao CF, Chen SY, Chen JY, Lee YHW. Modulation of p53 transcription regulatory activity and post-translational modification by hepatitis C virus core protein. *Oncogene* 2004; **23**: 2472–83.
37 Otsuka M, Kato N, Lan K *et al.* Hepatitis C virus core protein enhances p53 function through augmentation of DNA binding affinity and transcriptional ability. *J. Biol. Chem.* 2000; **275**: 34122–30.
38 Ray RB, Steele R, Meyer K, Ray R. Hepatitis C virus core protein represses p21WAF1/Cip1/Sid1 promoter activity. *Gene* 1998; **208**: 331–6.
39 Yamanaka T, Kodama T, Doi T. Subcellular localization of HCV core protein regulates its ability for p53 activation and p21 suppression. *Biochem. Biophys. Res. Commun.* 2002; **294**: 528–34.

40 Lee SK, Park SO, Joe CO, Kim YS. Interaction of HCV core protein with 14-3-3epsilon protein releases Bax to activate apoptosis. *Biochem. Biophys. Res. Commun.* 2007; **352**: 756–62.
41 Mohd-Ismail NK, Deng L, Sukumaran SK, Yu VC, Hotta H, Tan YJ. The hepatitis C virus core protein contains a BH3 domain that regulates apoptosis through specific interaction with human Mcl-1. *J. Virol.* 2009; **83**: 9993–10006.
42 Saito K, Meyer K, Warner R, Basu A, Ray RB, Ray R. Hepatitis C virus core protein inhibits tumor necrosis factor alpha-mediated apoptosis by a protective effect involving cellular FLICE inhibitory protein. *J. Virol.* 2006; **80**: 4372–9.
43 Tsutsumi T, Suzuki T, Moriya K *et al.* Hepatitis C virus core protein activates ERK and p38 MAPK in cooperation with ethanol in transgenic mice. *Hepatology* 2003; **38**: 820–8.
44 Matsuzaki K, Murata M, Yoshida K *et al.* Chronic inflammation associated with hepatitis C virus infection perturbs hepatic transforming growth factor beta signaling, promoting cirrhosis and hepatocellular carcinoma. *Hepatology* 2007; **46**: 48–57.
45 Wang XW, Hussain SP, Huo TI *et al.* Molecular pathogenesis of human hepatocellular carcinoma. *Toxicology* 2002; **181–182**: 43–7.
46 Tanji Y, Kaneko T, Satoh S, Shimotohno K. Phosphorylation of hepatitis C virus-encoded nonstructural protein NS5A. *J. Virol.* 1995; **69**: 3980–6.
47 De Mitri MS, Cassini R, Bagaglio S *et al.* Evolution of hepatitis C virus non-structural 5A gene in the progression of liver disease to hepatocellular carcinoma. *Liver Int.* 2007; **27**: 1126–33.
48 Kasprzak A, Adamek A. Role of hepatitis C virus proteins (C, NS3, NS5A) in hepatic oncogenesis. *Hepatol. Res.* 2008; **38**: 1–26.
49 Benga WJ, Krieger SE, Dimitrova M *et al.* Apolipoprotein E interacts with hepatitis C virus nonstructural protein 5A and determines assembly of infectious particles. *Hepatology* 2010; **51**: 43–53.
50 Kim K, Kim KH, Ha E, Park JY, Sakamoto N, Cheong J. Hepatitis C virus NS5A protein increases hepatic lipid accumulation via induction of activation and expression of PPARgamma. *FEBS Lett.* 2009; **583**: 2720–6.
51 Kato N, Lan KH, Ono-Nita SK, Shiratori Y, Omata M. Hepatitis C virus nonstructural region 5A protein is a potent transcriptional activator. *J. Virol.* 1997; **71**: 8856–9.
52 Lan KH, Sheu ML, Hwang SJ *et al.* HCV NS5A interacts with p53 and inhibits p53-mediated apoptosis. *Oncogene* 2002; **21**: 4801–11.
53 Majumder M, Ghosh AK, Steele R, Ray R, Ray RB. Hepatitis C virus NS5A physically associates with p53 and regulates p21/waf1 gene expression in a p53-dependent manner. *J. Virol.* 2001; **75**: 1401–7.
54 Chung YL, Sheu ML, Yen SH. Hepatitis C virus NS5A as a potential viral Bcl-2 homologue interacts with Bax and inhibits apoptosis in hepatocellular carcinoma. *Int. J. Cancer* 2003; **107**: 65–73.
55 He Y, Nakao H, Tan SL *et al.* Subversion of cell signaling pathways by hepatitis C virus nonstructural 5A protein via interaction with Grb2 and P85 phosphatidylinositol 3-kinase. *J. Virol.* 2002; **76**: 9207–17.
56 Park CY, Choi SH, Kang SM *et al.* Nonstructural 5A protein activates beta-catenin signaling cascades: implication of hepatitis C virus-induced liver pathogenesis. *J. Hepatol.* 2009; **51**: 853–64.
57 Peng L, Liang D, Tong W, Li J, Yuan Z. Hepatitis C virus NS5A activates the mammalian target of rapamycin (mTOR) pathway, contributing to cell survival by disrupting the interaction between FK506-binding protein 38 (FKBP38) and mTOR. *J. Biol. Chem.* 2010; **285**: 20870–81.
58 Yamashita T, Honda M, Kaneko S. Application of serial analysis of gene expression in cancer research. *Curr. Pharm. Biotechnol.* 2008; **9**: 375–82.
59 Honda M, Kaneko S, Kawai H, Shirota Y, Kobayashi K. Differential gene expression between chronic hepatitis B and C hepatic lesion. *Gastroenterology* 2001; **120**: 955–66.
60 Yamashita T, Kaneko S, Hashimoto S *et al.* Serial analysis of gene expression in chronic hepatitis C and hepatocellular carcinoma. *Biochem. Biophys. Res. Commun.* 2001; **282**: 647–54.
61 Okabe H, Satoh S, Kato T *et al.* Genome-wide analysis of gene expression in human hepatocellular carcinomas using cDNA microarray: identification of genes involved in viral carcinogenesis and tumor progression. *Cancer Res.* 2001; **61**: 2129–37.
62 Iizuka N, Oka M, Yamada-Okabe H *et al.* Comparison of gene expression profiles between hepatitis B virus- and hepatitis C virus-infected hepatocellular carcinoma by oligonucleotide microarray data on the basis of a supervised learning method. *Cancer Res.* 2002; **62**: 3939–44.
63 Honda M, Yamashita T, Ueda T, Takatori H, Nishino R, Kaneko S. Different signaling pathways in the livers of patients with chronic hepatitis B or chronic hepatitis C. *Hepatology* 2006; **44**: 1122–38.
64 Capurro M, Wanless IR, Sherman M *et al.* Glypican-3: a novel serum and histochemical marker for hepatocellular carcinoma. *Gastroenterology* 2003; **125**: 89–97.
65 Jia HL, Ye QH, Qin LX *et al.* Gene expression profiling reveals potential biomarkers of human hepatocellular carcinoma. *Clin. Cancer Res.* 2007; **13**: 1133–9.
66 Llovet JM, Chen Y, Wurmbach E *et al.* A molecular signature to discriminate dysplastic nodules from early hepatocellular carcinoma in HCV cirrhosis. *Gastroenterology* 2006; **131**: 1758–67.
67 Wurmbach E, Chen YB, Khitrov G *et al.* Genome-wide molecular profiles of HCV-induced dysplasia and hepatocellular carcinoma. *Hepatology* 2007; **45**: 938–47.
68 Jopling CL, Yi M, Lancaster AM, Lemon SM, Sarnow P. Modulation of hepatitis C virus RNA abundance by a liver-specific MicroRNA. *Science* 2005; **309**: 1577–81.
69 Murakami Y, Aly HH, Tajima A, Inoue I, Shimotohno K. Regulation of the hepatitis C virus genome replication by miR-199a. *J. Hepatol.* 2009; **50**: 453–60.
70 Sarasin-Filipowicz M, Krol J, Markiewicz I, Heim MH, Filipowicz W. Decreased levels of microRNA miR-122 in individuals with hepatitis C responding poorly to interferon therapy. *Nat. Med.* 2009; **15**: 31–3.
71 Pedersen IM, Cheng G, Wieland S *et al.* Interferon modulation of cellular microRNAs as an antiviral mechanism. *Nature* 2007; **449**: 919–22.
72 Braconi C, Valeri N, Gasparini P *et al.* Hepatitis C virus proteins modulate microRNA expression and chemosensitivity in malignant hepatocytes. *Clin. Cancer Res.* 2010; **16**: 957–66.
73 Banaudha K, Kaliszewski M, Korolnek T *et al.* MicroRNA silencing of tumor suppressor DLC-1 promotes efficient hepatitis C virus replication in primary human hepatocytes. *Hepatology* 2011; **53**: 53–61.
74 Ura S, Honda M, Yamashita T *et al.* Differential microRNA expression between hepatitis B and hepatitis C leading disease progression to hepatocellular carcinoma. *Hepatology* 2009; **49**: 1098–112.
75 Wong QW, Lung RW, Law PT *et al.* MicroRNA-223 is commonly repressed in hepatocellular carcinoma and potentiates expression of Stathmin1. *Gastroenterology* 2008; **135**: 257–69.

UICC
global cancer control

IJC
International Journal of Cancer

Identification of a secretory protein c19orf10 activated in hepatocellular carcinoma

Hajime Sunagozaka, Masao Honda, Taro Yamashita, Ryuhei Nishino, Hajime Takatori, Kuniaki Arai, Tatsuya Yamashita, Yoshio Sakai and Shuichi Kaneko

Department of Gastroenterology, Kanazawa University Hospital, Kanazawa, Ishikawa, Japan

The identification of genes involved in tumor growth is crucial for the development of inventive anticancer treatments. Here, we have cloned a 17-kDa secretory protein encoded by *c19orf10* from hepatocellular carcinoma (HCC) serial analysis of gene expression libraries. Gene expression analysis indicated that *c19orf10* was overexpressed in approximately two-thirds of HCC tissues compared to the adjacent noncancerous liver tissues, and its expression was significantly positively correlated with that of alpha-fetoprotein (AFP). Overexpression of *c19orf10* enhanced cell proliferation of AFP-negative HLE cells, whereas knockdown of *c19orf10* inhibited cell proliferation of AFP-positive Hep3B and HuH7 cells along with G1 cell cycle arrest. Supplementation of recombinant c19orf10 protein in culture media enhanced cell proliferation in HLE cells, and this effect was abolished by the addition of antibodies developed against c19orf10. Intriguingly, c19orf10 could regulate cell proliferation through the activation of Akt/mitogen-activated protein kinase pathways. Taken together, these data suggest that c19orf10 might be one of the growth factors and potential molecular targets activated in HCC.

Hepatocellular carcinoma (HCC) is one of the most common cancers with an estimated worldwide incidence of 1,000,000 cases per year.[1] Most HCCs develop as a consequence of chronic liver disease such as chronic viral hepatitis due to hepatitis C virus (HCV) or hepatitis B virus (HBV) infection.[2–7] Liver cirrhosis patients with any etiology are considered to be at an extremely high risk for HCC.[8–10] Indeed, ~7% of liver cirrhosis patients with HCV infection develop HCC annually,[8,11] and the advancement of reliable HCC screening methods for high-risk patients is crucial for the improvement of their overall survival.[12]

Currently, imaging diagnostic techniques such as ultrasonography, computed tomography, magnetic resonance image and angiography are the gold standards for the early detection of HCC.[13,14] In addition, tumor markers such as alpha-fetoprotein (AFP) and des-gamma carboxyl prothrombin (DCP) have been used for the screening of HCC,[15–18] although their sensitivity and specificity are not sufficiently high. Recently, a gene expression profiling approach shed new light on Glypican 3, a heparin sulfate proteoglycan anchored to the plasma membrane, as a potential HCC marker, and its clinical usefulness as a molecular target as well as a tumor marker is presently under investigation.[19]

There are several options available for the treatment of HCC, including surgical resection, liver transplantation, radiofrequency ablation, transcatheter arterial chemoembolization and chemotherapy, while taking the HCC stage and liver function into consideration. Recently, molecular therapy targeting the Raf kinase/vascular endothelial growth factor receptor (VEGFR) kinase inhibitor sorafenib improved the survival of patients with advanced HCC,[20,21] emphasizing the importance of deciphering the molecular pathogenesis of HCC for the development of effective treatment options.

Here, we investigated the gene expression profiles of HCC by serial analysis of gene expression (SAGE) to discover a novel gene activated in HCC.[22–25] We identified a gene, *c19orf10*, overexpressed in HCC and determined that the encoded 17-kDa protein (c19orf10) is a secretory protein. Murine *c19orf10* was originally discovered to encode a cytokine interleukin (IL)-25/stroma-derived growth factor (SF20) in 2001.[26] The gene *c19orf10* was mapped in the H2 complex region of mouse chromosome 17 between *C3* and *Ir5*, and the hypothetical protein was predicted as globular protein.[26] However, the subsequent study failed to reproduce its proliferative effect on lymphoid cells, and the paper was retracted by the authors in 2003.[26,27] Nevertheless, independent studies revealed that c19orf10 was indeed produced by synoviocytes, macrophages and adipocytes, although the function of c19orf10 remained elusive.[28,29] In our study, we identified that *c19orf10* was overexpressed in AFP-positive HCC samples. Our data imply that c19orf10 could activate the mitogen-activated protein kinase (MAPK)/Akt pathway and

Key words: hepatocellular carcinoma, serial analysis of gene expression, *c19orf10*
Additional Supporting Information may be found in the online version of this article
DOI: 10.1002/ijc.25830
History: Received 14 Mar 2010; Accepted 15 Nov 2010; Online 2 Dec 2010
Correspondence to: Shuichi Kaneko, Kanazawa University Hospital, 13-1 Takara-machi, Kanazawa, Ishikawa 920-8641, Japan,
Tel.: +81-76-265-2233, Fax: +81-76-234-4250,
E-mail: skaneko@m-kanazawa.jp

enhance cell proliferation in HCC cell lines, suggesting that c19orf10 may be a growth factor produced by tumor epithelial cells and/or stromal cells, and, therefore, would be a good target for the treatment of HCC.

Material and Methods

SAGE and HCC samples

HCC and normal liver SAGE libraries that we had constructed were reanalyzed using SAGE 2000 software. The size of each SAGE library was normalized to 300,000 transcripts per library. Monte Carlo simulation was used to select genes whose expression levels were significantly different between the two libraries. Each SAGE tag was annotated using the gene-mapping website SAGE Genie database (http://cgap.nci.nih.gov/SAGE/) and the SOURCE database (http://smd.stanford.edu/cgi-bin/source/sourceSearch) as previously described.[30] An additional 15 SAGE libraries of normal and cancerous tissues from various organs were retrieved using the National Center for Biotechnology Information SAGEmap (http://www.ncbi.nlm.nih.gov/SAGE/).

Fifteen HCC tissues (four HBV-related and 11 HCV-related) and the corresponding noncancerous liver tissues were obtained from HCC patients who received hepatectomy. Four normal liver tissues were obtained from patients undergoing surgical resection of the liver for the treatment of metastatic colon cancer. Additionally, 36 HCC tissues (17 HBV-related and 19 HCV-related) were obtained from HCC patients undergoing hepatectomy. These samples were snap frozen in liquid nitrogen immediately after resection and used for quantitative real-time detection PCR (RTD-PCR). Total RNA was extracted using a ToTALLY RNA™ kit (Ambion, Austin, TX).

The study protocol conformed to the ethical guidelines of the Declaration of Helsinki (1975) and was approved by the institutional ethical review board committee. All patients provided written informed consent for the analysis of the specimens.

Laser capture microdissection and RNA isolation

Laser capture microdissection (LCM) was performed as previously described.[31] Briefly, 20 HCV-related surgically resected HCC tissues were frozen in OCT compound (Sakura Finetech, Torrance, CA).[32] Inflammatory cells and cancerous cells in HCC tissues were separately excised by LCM using a Laser Scissors CRI-337 (Cell Robotics, Albuquerque, NM) under a microscope. Total RNA was isolated from these cells using a microRNA isolation kit (Stratagene, La Jolla, CA) in accordance with the supplied protocol, with slight modifications.[31]

Construction of C19ORF10 expression plasmid and recombinant adenovirus vector

PCR was performed on a Marathon cDNA library from Huh7 cells using the following primers: sense primers: 5′-GACCCTAGTCCAACATGGCGGCGCCC-3′ (the first PCR), 5′-ATGGCGGCGCCCAGCGGAGGGTGGAACGGC-3′ (the nested second PCR) and antisense primers: 5′-CACCGGA GATGAGAAGGTGCCACCCGC-3′ (the first PCR), 5′-CAG GGCTGCTGGTCACAGCTCAGTGCGCG-3′ (the nested second PCR). The 5′ and 3′ends of the cDNA were isolated using a SMART RACE cDNA Amplification kit (Clontech, Mountain View, CA) according to the manufacturer's recommendations. The PCR products were cloned into a TA vector (Invitrogen, Carlsbad, CA) to generate the pcDNA3.1-*c19orf10* expression plasmid. Using this plasmid, a C-terminally FLAG-tagged construct of *c19orf10* was generated and inserted in a pSI mammalian expression vector (Promega, Madison, WI), which was driven by the SV40 promoter (pSI-*c19orf10*).

The replication-incompetent recombinant adenovirus vector expressing FLAG-tagged *c19orf10* (Ad. *c19orf10-FLAG*) was generated by homologous recombination using the AdMax system (Microbix, Toronto, Canada) as previously described.[33] The generated recombinant adenovirus was purified by limiting dilution, and the titer of viral aliquots was determined by the 50% tissue culture infectious dose method as previously described.[34]

RTD-PCR

RTD-PCR was performed as previously described.[31] Briefly, template cDNA was synthesized from 1 μg of total RNA using SuperScript™ II RT (Invitrogen). RTD-PCR of *c19orf10* (Hs. 00384077_m1), *AFP* (Hs00173490_m1), *GPC3* (Hs01018938_m1), *KRT19* (Hs00761767_s1) and the *ACTB* internal control (Hs99999903_m1) was performed using a TaqMan® Gene Expression Assay kit (Applied Biosystems, Foster City, CA). The expression of selected genes was measured in triplicate by ΔΔCT method using the 7900 Sequence Detection System (Applied Biosystems).

Cell lines and transfection of plasmids

Human liver cancer cell lines HuH1, Huh7, Hep3B, HLE and HLF as well as HEK293 and NIH3T3 were cultured in Dulbecco's modified Eagle's medium (Invitrogen) supplemented with 10% heat-inactivated fetal bovine serum (Invitrogen) in 5% CO_2 at 37°C. Transfection of plasmids was performed using FuGENE™ 6 (Roche Diagnostics, Indianapolis, IN) according to the manufacturer's instruction. Briefly, 5×10^5 cells were seeded in a six-well plate 12 hr before transfection, and 3 μg of plasmid DNA was used for each transfection. All experiments were repeated at least twice.

Purification of c19orf10-FLAG fused protein and production of anti-c19orf10 antibody

Approximately 500 ml of culture supernatant obtained from HEK293 cells infected with Ad. *C19ORF10-FLAG* at a multiplicity of infection of 20 was applied to an anti-FLAG affinity gel column (Sigma-Aldrich, St. Louis, MO). The column was

Table 1. ESTs overexpressed in the HCC library

Tag sequence	p value	HCC	Normal liver	T/N ratio	Name	UniGene ID
TGGGCAGGTG	<0.00001	33	0	>33	Chromosome 5 open reading frame 13	Hs.483067
GCAAAATATC	<0.00001	31	2	15.5	Liver cancer-associated noncoding mRNA, partial sequence	Hs.214343
AGCCTGCAGA	0.0002	12	1	12	Chromosome 19 open reading frame 10	Hs.465645
TTGTGCACGT	0.000228	12	1	12	CDNA FLJ45284 fis, clone BRHIP3001964	Hs.514273
ACATTCTTGT	0.000042	12	0	>12	Transcribed locus, strongly similar to XP_496055.1	Hs.76704
ACAAGTACCC	0.001161	10	1	>10	Chromosome 5 open reading frame 13	Hs.483067
GAGGTGAAGG	0.000174	10	0	>10	KIAA1914	Hs.501106
GCTGGAGGAG	0.000114	10	0	>10	Transcribed locus	Hs.520115

subjected to elution by competition with FLAG peptide (5 μg/ml), and each 1 ml fraction of the eluted aliquot was collected to obtain the most concentrated c19orf10-FLAG protein in accordance with the manufacturer's protocol. The anti-c19orf10 antibodies were developed by immunizing rabbits with repeated intradermal injections of purified c19orf10-FLAG. Protein concentration was measured by the Bradford method.

Silencing gene expression by short interfering RNA

The selected short interfering RNA (siRNA) targeting *C19ORF10* (Si-*C19ORF10*; Silencer Select siRNAs s31855) and the irrelevant control sequence (Si-*Control*; Silencer Select siRNAs 4390843) was obtained from Applied Biosystems. Transfection of these siRNAs was performed using FuGENE™ 6 (Roche Diagnostics) as previously described.[30] Briefly, 2×10^5 cells were seeded in a six-well plate 12 hr before transfection. A total of 100 pmol/l of siRNA duplex was used for each transfection. The experiments were performed at least twice.

Cell proliferation assay

Cell proliferation was evaluated in quadruplicate using a Cell Titer 96 MTS Assay kit (Promega). Briefly, 2×10^3 HLE or HuH7 cells were harvested in a 96-well plate 12 hr before the transfection or addition of the recombinant proteins. Transfection of siRNAs or plasmids was performed using FuGENE™ 6 (Roche Diagnostics). After incubation with MTS/PMS solution at 37°C for 2 hr, the absorbance at 450 nm was measured. The experiments were performed at least twice.

Cell cycle analysis

Cells were fixed using 80% ice-cold ethanol and incubated with propidium iodide for 10 min. DNA content was analyzed using a FACS Caliber flow cytometer (BD Biosciences, San Jose, CA) counting 10,000 stained cells. The distribution of cells in each cell cycle phase was determined using FlowJo software (Tree Star, Ashland, OR).

Western blotting

Cells were lysed in radioimmunoprecipitation assay (RIPA) buffer, and the extracts were subsequently electrophoresed on sodium dodecyl sulfate–10% polyacrylamide gels and transferred onto protean nitrocellulose membranes. The blots were then incubated for 1 hr with an appropriate primary monoclonal antibody: phospho-PI3K (#4228), phospho-Akt (#4060), phospho-GSK-3β (#9323), phospho-c-Raf (#9427), phospho-MEK1/2 (#9154), phospho-p44/42 MAPK (Erk1/2) (#4370), Cdk4 (CDK4 (#2906)), Cdk6 (#3136), cyclinD1 (#2926), cyclinD3 (#2936), phospho-Rb (#9308), phospho-P53 (# 9286), phospho-cdc2 (#9111) and β-actin (#4970) (Cell Signaling Technology, Allschwil, Switzerland) and anti-FLAG antibodies (Sigma-Aldrich, St. Louis, MO). The blots were washed and exposed to peroxidase-conjugated secondary antibodies, such as anti-mouse or rabbit IgG antibodies, and visualized using the ECL™ kit (Amersham Biosciences, Piscataway, NJ). All experiments were performed at least twice.

Statistical analyses

Unpaired *t*-tests and Kruskal–Wallis tests were performed on the RTD-PCR and cell proliferation data using GraphPad Prism software (www.graphpad.com).

Results

Identification of *C19ORF10* overexpression in HCC by SAGE

To comprehensively explore the candidate novel genes activated in HCC, we reanalyzed two SAGE libraries derived from HCC tissues and normal liver tissues.[30] After normalization of each SAGE library size to 300,000 tags, we compared the HCC and normal liver libraries to obtain the list of genes overexpressed in HCC. We identified 79 genes significantly overexpressed in the HCC library by more than tenfold when compared to the normal liver library (Supporting Information Table 1). Among them, we explored expressed sequence tags (ESTs) as candidates for novel HCC-related genes to identify eight unique tags corresponding to seven ESTs (Table 1). We especially focused on the EST chromosome 19 open reading frame 10 (*c19orf10*) because the